Thermal Science and Engineering 2026, 9(2), 026100001.
https://doi.org/10.24294/tse026100001

Review

Applicable methodologies for modelling of heat and mass transfer phenomena in tumble dryers: A review

Sajad Salavati[1,2], Arash Hajisharifi[1], Michele Girfoglio[1], Giovanni Stabile[3], Gianluigi Rozza[1,*]

[1] Mathematics Area, MathLab, International School for Advanced Studies (SISSA), via Bonomea 265, I-34136 Trieste, Italy
[2] Department of Electrical and Computer Engineering, Aarhus University, 8200 Aarhus N, Denmark
[3] Department of Pure and Applied Sciences, Informatics and Mathematics Section, University of Urbino Carlo Bo, Piazza della Repubblica 13, I-61029 Urbino, Italy
*** Corresponding author:** Gianluigi Rozza, grozza@sissa.it

CITATION

Salavadezfouli S, Hajisharifi A, Girfoglio M, et al. Applicable methodologies for modelling of heat and mass transfer phenomena in tumble dryers: A review. Thermal Science and Engineering. 2026; 9(2): 026100001. https://doi.org/10.24294/tse026100001

ARTICLE INFO

Received: 23 March 2024
Accepted: 13 May 2026
Available online: 27 July 2026

COPYRIGHT

Copyright © 2026 by author(s). *Thermal Science and Engineering* is published by EnPress Publisher, LLC. This work is licensed under the Creative Commons Attribution (CC BY) license. https://creativecommons.org/licenses/by/4.0/

Abstract: Tumble dryers are convenient but energy-intensive, and their performance depends on coupled heat and mass transfer within the drum and air circuit. This review evaluates mathematical modeling approaches for these processes, spanning 0-D lumped-parameter models, 1-D heat and moisture transfer models, and kinematic and image-processing methods, across vented, condenser, and heat-pump dryer types. Literature was drawn from peer-reviewed sources published roughly since the 1990s. The Chilton–Colburn analogy remains the dominant framework for evaporation-rate modeling, but its reliance on constant transfer coefficients, uniform textile temperature, and saturated surface assumptions limits its accuracy during the falling-rate drying period, when evaporation slows and a larger fraction of supplied energy may be diverted to heating the textiles and drum rather than moisture removal. This review's contribution lies in systematically comparing classical models (Lambert, Deans) against newer 1-D, regression-based, kinematic, and image-processing strategies, clarifying the assumptions, applicability boundaries, and engineering trade-offs of each. The findings point toward hybrid, uncertainty-aware models that couple energy-balance formulations with variable transfer coefficients, textile-motion data, and data-driven tools as the most promising path forward for energy-efficient dryer design and control.

Keywords: tumble dryer; evaporation rate; area-mass transfer coefficient; review

1. Introduction

Growing concerns about the efficient use of energy resources, together with the need to meet climate change targets, have led to a focus on energy-intensive technologies, such as drying [1–6]. Drying (also termed dehydration or dewatering) involves lowering the moisture content of a material to a specified level without impairing the product's quality or structural integrity [7,8]. Although drying was traditionally carried out under sunny and windy conditions, today limited space, tighter production schedules, and the demand for faster and more controllable processing have driven the shift toward artificial drying methods [9]. For this reason, drying is now integral to many domestic and industrial activities, including food processing, textiles, paper, wood, ceramics, minerals, pharmaceuticals, HVAC and ventilation systems [10–21]. From an energy standpoint, drying is among the most demanding unit operations in process industries, accounting for up to about 25% of total industrial energy use in this sector [22,23]. Yet, widely used conventional dryers often have short service lives and require substantial energy and operating costs. These limitations are increasingly difficult to justify under current conditions, where industry is expected to respond to the global energy situation, reduce lifecycle costs, and adopt more environmentally responsible technologies [24].

Industrial drying was initially introduced in the field of chemical engineering a few decades ago [25]. This technology has since found diverse applications, with one of the main uses being the drying of porous fabrics, including clothes. The use of domestic tumble clothes dryers has been growing continuously for decades [26]. Drying is one of the most energy-consuming processes [27]. According to a Department of Energy chart (**Figure 1**), the clothes dryer consumes the second largest amount of electricity among household appliances, after the water heater [28]. This is quite a bit of electricity use for an appliance that is only run once or twice a week, as compared to an appliance that is running constantly. Clothes dryers have become standard household appliances in many parts of the world because they provide reliable and fast drying systems [29,30]. Currently, more than 40% of households in Germany and over 80% in the United States own a clothes dryer, and the global market continues to expand steadily [31]. Despite their convenience, the main drawback of these systems is their substantial electricity consumption [32]. It is estimated that clothes dryers account for more than 3% of residential energy use in the United States, while their contribution is approximately 8% in the world [33,34]. The use of tumble dryers has been increasing at an annual growth rate of about 10.9%, driven by changes in living environments and consumption patterns, reduced living space, rising environmental concerns, increased awareness of hygiene, since sun-drying eliminates only a limited portion of bacteria, and continuous improvements in fabric-care technologies [35]. Nevertheless, fabric drying remains both energy-intensive and time-consuming, often requiring up to three hours depending on operating conditions and dryer type. At the same time, the ongoing energy crisis and growing environmental awareness have intensified public and industrial interest in energy-efficient solutions. Consequently, manufacturers are increasingly focused on enhancing the energy performance of drying systems to maintain market competitiveness, sustain sales growth, and support long-term sustainability objectives [3,36,37].

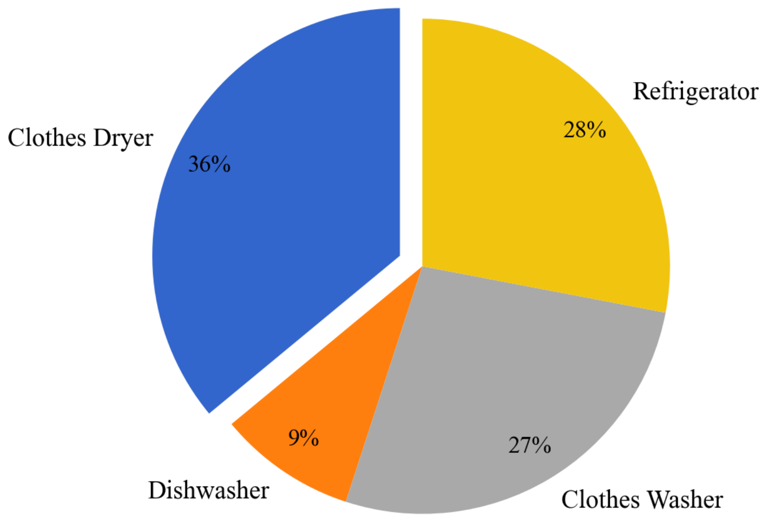

Figure 1. Energy consumption of standard home appliances [28].

Clothes dryers operate by passing heated air through a rotating drum that contains the textiles, allowing the air to absorb moisture and carry it away. Depending on the operating cycle and energy supply, tumble dryers are commonly grouped into two main types [38]. In vented dryers, the process follows an open cycle: heated air flows through the drum, removes moisture from the fabrics, and is then discharged into the surrounding environment [39]. By contrast, condenser dryers operate in a closed air loop, where the moist air leaving the drum is cooled in a condenser so that the water vapor condenses and is removed before the air is reheated and circulated again [40]. The configurations of these systems are illustrated in **Figures 2** and **3**.

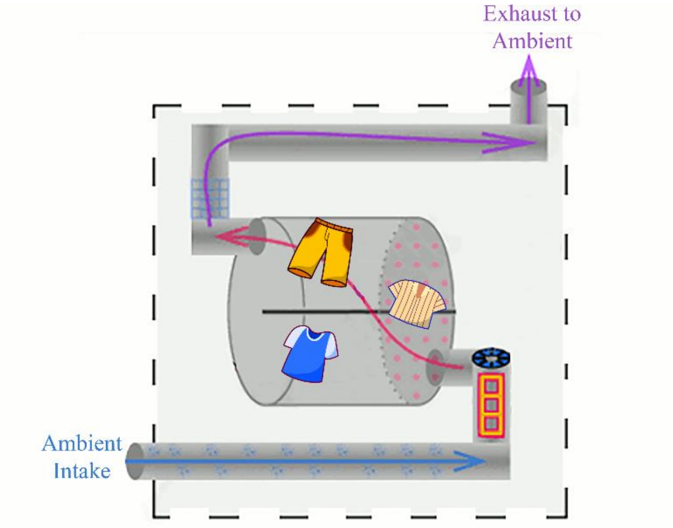

Figure 2. Schematic of drying cycle of the vented dryers.

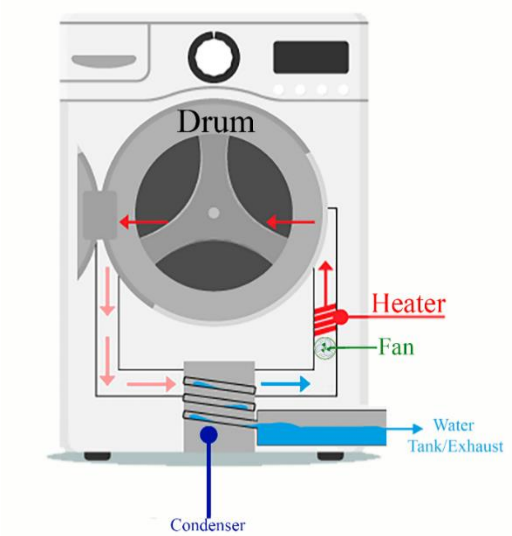

Figure 3. Schematic of a drying cycle of the condenser dryers.

In vented dryers, the hot air is typically produced either by a gas burner or by an electric heating element, whereas condenser dryers generally rely on electrical heating. More recent designs, known as heat pump dryers, incorporate a heat pump cycle that allows part of the thermal energy to be recovered and reused within the system, thereby improving overall efficiency [41]. Because of the interaction between the refrigeration loop and the drying air loop, these dryers are considered relatively complex systems. In practice, they consist of two coupled closed circuits: a refrigerant cycle, often using R134a as the working fluid [42–46], and a drying air circuit that contains the air–moisture mixture. Heat transfer between the two circuits takes place in the condenser and evaporator, as shown in **Figure 4** [47].

The vented and heat-pump dryers are generally sold as separate appliances, so they must be installed alongside the washing machine and therefore take up extra space [48,49]. Condenser dryers, in contrast, are often used in combined units where washing and drying are performed in the same machine (washer–dryers), which makes them more practical for homes. In these appliances, the humid air leaving the drum is cooled—typically by ambient air or by water, so that the moisture condenses and can be removed. Because this configuration avoids the need for an additional standalone dryer and can reduce both energy use and drying time, condenser-based systems have become widely adopted and represent a substantial share of the U.S. market [50].

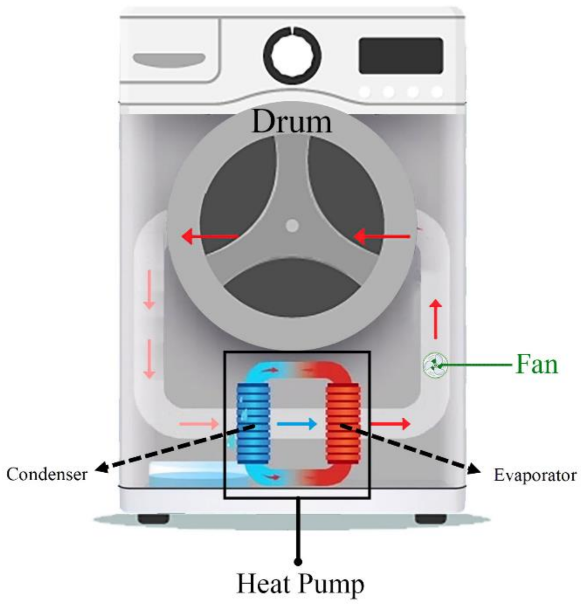

Figure 4. Schematic of a drying cycle of the heat pump dryers.

The study of physical phenomena in tumble dryers has gained considerable attention in recent years. A multitude of studies have contributed to the understanding of these complex systems [51–53]. Sousa et al. focused on the distribution of the moisture in the textile sheets and discovered that the moisture variation in the samples occurred uniformly in position and time [54]. Researchers have also addressed the challenges posed by energy consumption and drying efficiency [55–58]. For instance, Cay et al. conducted a study in which they explored dryer performance parameters through exergy analysis and mathematical models [59,60]. That resulted in a correlation between the dryer efficiency and exergy. Various computer models have been proposed through the years for evaluating the performance indices of clothes dryers [61,62]. The contributions have laid the foundation for our exploration of applicable methodologies in this paper, as we seek to build upon and extend the existing knowledge in the field.

To encapsulate, the energy-intensive nature of drying processes, particularly in the case of tumble dryers, poses significant challenges in the context of today's global energy crisis and the urgent need for a sustainable, environmentally friendly technology. Indeed, as the second-largest consumer of electricity among household appliances, tumble dryers are both ubiquitous and resource-intensive. The increasing adoption of these home appliances worldwide, driven by changes in consumption patterns and living conditions, necessitates the employment of innovative solutions to improve energy efficiency while maintaining effective drying performance.

The aim of this review goes beyond cataloging existing tumble-dryer models. Rather, it seeks to classify them according to the physical assumptions they rely on, the inputs they require, their suitability for different dryer configurations, and their practical usefulness for engineering design. Unlike previous reviews, which have tended to focus on overall dryer performance or energy-saving technologies, the present work centers specifically on evaporation-rate modeling and the role of heat and mass transfer assumptions in shaping model behavior and reliability. In doing so, it examines where the constant evaporation-rate and constant area–mass transfer coefficient assumptions hold and where they break down, compares lumped, one-dimensional, regression-based, physics-based, and kinematic modeling strategies side by side, and identifies the main sources of uncertainty that limit how freely models can be transferred between vented, condenser, and heat-pump dryer types.

2. Review methodology and scope

The literature for this review was gathered from peer-reviewed journal papers, conference articles, technical reports, and relevant standards published since the 1990s. The primary databases searched were Scopus, Web of Science, ScienceDirect, IEEE Xplore, and Google Scholar, using keywords including: *tumble dryer modeling; clothes dryer evaporation rate; heat and mass transfer in textile drying; area–mass transfer coefficient; Chilton–Colburn analogy; dryer SMER; heat-pump clothes dryer;* and *fabric motion in tumble dryers*.

Studies were included when they presented mathematical, numerical, experimental, or semi-empirical approaches to predicting dryer performance, evaporation rate, textile moisture content, air temperature, humidity ratio, SMER, or drying time. Work dealing exclusively with general industrial drying was drawn upon only where it provided directly relevant heat and mass transfer concepts. Throughout, the review focuses on domestic vented, condenser, and heat-pump tumble dryers, with particular attention to modeling assumptions, applicability conditions, sources of uncertainty, and practical engineering usefulness.

3. Physical phenomena

This section examines the drying loop of a condenser tumble dryer (**Figure 5**). The loop is made up of four main components: the fan, heater, drum, and condenser. The fan's role is to drive the air-vapor mixture around the circuit; it is usually assumed not to change the mixture's thermodynamic state. The main thermodynamic changes occur in the remaining components. In most dryer designs, the heater is in the air duct close to the fan (typically downstream of the impeller), and it is therefore convenient to treat the fan and heater as a single stage. With this simplification, the cycle can be described using three state points (labeled a, b, and c in **Figure 5**), each representing the air condition after a major component. The key variables used to describe the air state are the dry-bulb temperature, the humidity ratio (absolute humidity), and the relative humidity. Under idealized operation, their evolution through the cycle can be summarized as follows.

- Fan/Heater ($a -> b$): While the heat increases the air temperature, the humidity ratio remains constant as no phase change occurs in this section. On the psychrometric chart (**Figure 6**), this corresponds to an approximately horizontal shift from point *a* to point *b*.
- Drum ($b -> c$): The hot air evaporates the moisture into the airflow as it passes through the wet textiles. Evaporation removes heat from the air–fabric system, so the air temperature drops. At the same time, both the humidity ratio and the relative humidity rise, approaching saturation. In the ideal case, the air leaving the drum is expected to be fully saturated (relative humidity ≈ 100%) [63,64]. In real machines, however, saturation is not always reached, particularly during the middle and final stages of drying, so the outlet state follows a non-saturated path, as indicated by the solid curve in **Figure 6** rather than the idealized dotted trajectory [65].
- Condenser ($c -> a$): In the condenser, the humid air is cooled, and part of its water vapour condenses out. This section is commonly represented as cooling with condensation occurring while the air remains close to saturation, corresponding to the path from *c* back to *a* in **Figure 6**.

The overall changes of the thermodynamic variables across the modules are summarized in **Table 1**.

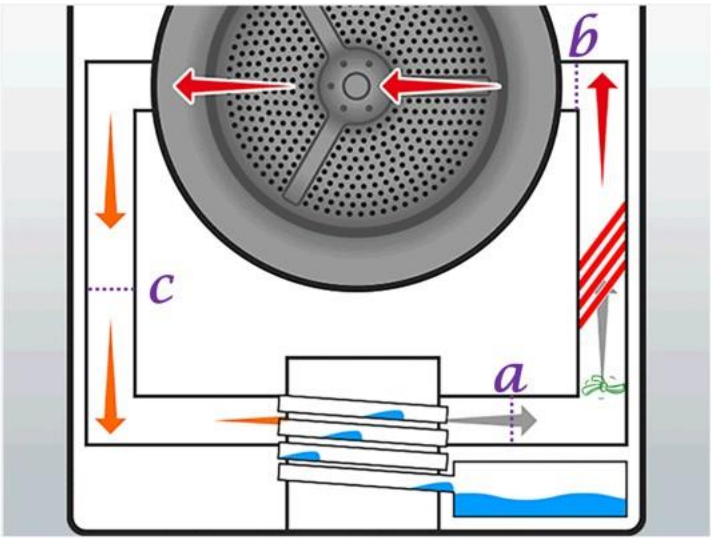

Figure 5. Different sections in the drying cycle of the condenser dryer.

Table 1. Thermodynamic changes of the mixture in the cycle.

Module	**Fan/heater**	**Drum**	**Condenser**
Path	a –> b	b –> c	c –> a
Dry Bulb Temp.	T_{dry} ↑	T_{dry} ↓	T_{dry} ↓
Relative Humidity	RH↓	RH↑	RH≃
Absolute Humidity	AH≃	AH↑	AH↓

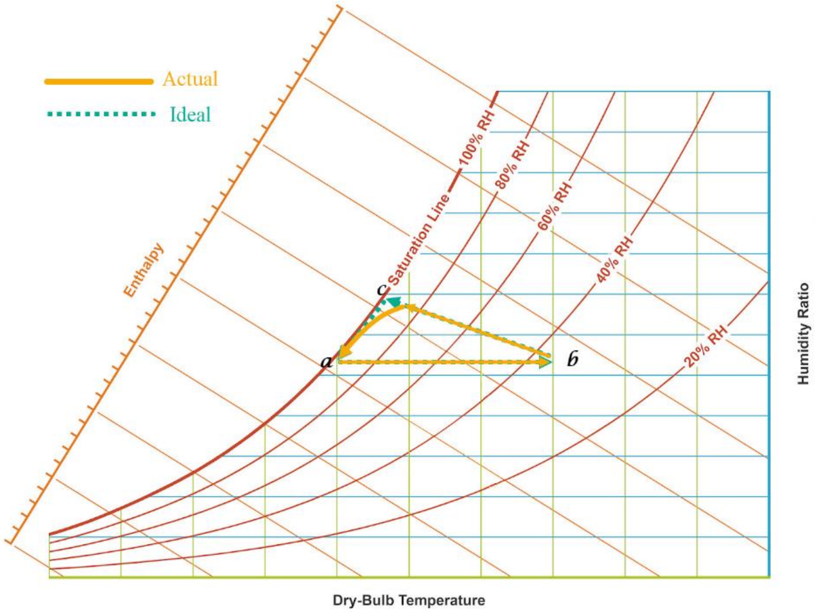

Figure 6. Ideal drying cycle in the psychometric chart.

Beyond these bulk thermodynamic trends, several coupled physical processes take place inside the dryer, involving both the air–vapor mixture and the textiles. While the drum rotates and the load tumbles, hot, relatively dry air enters the drum, mixes with the wet fabrics, and flows through the porous textile structure. Heat and mass transfer occur simultaneously: heat is exchanged by conduction within and between fabric layers and by convection between the fabric surfaces and the flowing air, while radiative exchange occurs among internal components throughout the dryer. Mass transfer is responsible for moisture evaporation from the textiles within the drum and for subsequent condensation of moisture from the airflow in the condenser. The system's behavior is further complicated by transient operation, such as heater cycling used to regulate the drying temperature, and by the continually changing, largely random configuration of the fabric load as it tumbles. The main phenomena and their associated locations within the dryer are summarized in **Table 2**.

Finally, the motion of items inside the rotating drum can exhibit distinct two-phase flow regimes. Jones et al. identified six regimes that depend on the Froude number, $Fr = \omega^2 R/g$, in the drum, where ω, R and g are the drum's angular speed, drum radius and gravitational acceleration, respectively [66]. The range of fabric motions associated with these regimes is illustrated in **Figure 7**.

Froude number is the ratio of inertial (here the centripetal) to gravitational forces. Flows with higher Froude numbers, i.e., a large diameter or a fast angular speed, tend to form a cascading or cataracting motion ($Fr \simeq 0.1 \sim 0.5$). At $Fr > 1$, the flow exhibits a complete centrifuging motion as centripetal forces become dominant. In these final regimes, the assumption of static flow in the bed is no longer valid, in which the media is flung a greater distance across the drum [67,68].

Clearly, the most evaporation occurs during the free-fall period, when there is extensive contact between the liquid and gas phases. This maximizes the heat transfer rate between the hot air and the wet media [69]. As a result, to ensure a maximum mass transfer rate, the Froude number must be chosen to guarantee the cataracting regime. Switching to the centrifuging or cascading regimes reduces the rate of evaporation accordingly. However, the cataracting and cascading regimes cause more damage to the fabrics than centrifuging over the drying cycle [69].

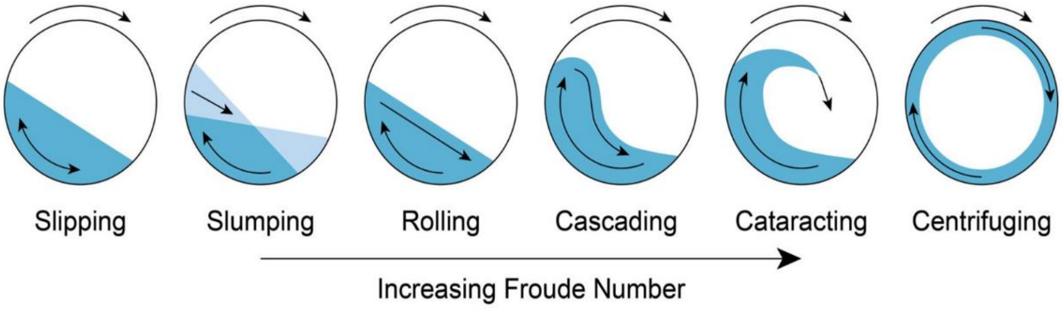

Figure 7. Flow regimes in rotating drums as a function of Froude number [69].

Table 2. Physical phenomena.

Phenomenon	Module
Multi-component flow (air and vapor)	Fan/Heater, Drum, Condenser
Multi-body dynamics (MBD) (clothes rotation)	Drum
Heat transfer (convection and radiation)	Fan/Heater, Drum, Condenser
Heat Transfer (conduction between clothes)	Drum
Variable thermophysical properties	Fan/Heater, Drum
Multiphase flow (gas and water)	Drum, Condenser
Mass Transfer (evaporation and condensation)	Drum, Condenser

In summary, the physical phenomena within the condenser dryer include simultaneous heat and mass transfer mechanisms, all occurring within the dynamic environment of the drum. As hot, dry air enters the drum and mixes with the wet clothes, a series of processes occur. Conductive and convective heat transfers between the clothes and air, along with radiation between various components within the dryer, contribute to the heat transfer dynamics. On the other hand, the mass transfer process drives the evaporation of moisture from the clothes into the air, followed by air condensation in the condenser. These processes are further complicated by the intermittent operation of the heater to maintain a constant drying temperature and the unpredictable movement of clothes within the drum.

It should be noted that although both mass and heat transfer occur in the system, there is a direct connection between these processes. Specifically, when dealing with the phenomenon of evaporation, a fundamental relationship arises through the following relation:

$$Q = \dot{m}_{evap}/h_{fg} \tag{1}$$

where Q represents the heat transfer rate, $\dot{m}_{evap}$ is the evaporated mass and h_{fg} is the latent heat of vaporization. As a result, the main focus can be directed to the calculation and analysis of mass transfer phenomena. Understanding this complex phenomenon is vital for optimizing the performance of the condenser dryers.

In the subsequent sections, the focus is on the methodologies for estimating system variables, including temperature, humidity, and airflow, as well as the crucial parameter of evaporation rate. The goal is to provide valuable insights into the mass transfer phenomenon within tumble dryers and contribute to the development of energy-efficient and sustainable drying technologies by comprehensively examining these aspects.

4. Modeling methodologies

There has been limited literature on laundry drying technologies, especially tumble dryers, before the 1990s, with early studies primarily focused on drying textiles during the manufacturing process [70]. The initial exploration of the tumble dryer's drum module began with observational studies and experimental measurements [71,72]. One of the earliest notable studies was conducted by Hekmat et al. [73], which introduced practical methods, including reducing airflow rates and recirculating exhaust air, aimed at improving drying efficiency. These methods showed potential for achieving up to a 33% reduction in energy consumption, albeit at the cost of a longer drying time [74]. Another pivotal study by Spruit et al. [75] involved measuring temperature and humidity changes within the drum to assess drying performance. Remarkably, they discovered that increasing the textile load by 20% above the nominal load resulted in a significant 66% improvement in drying efficiency in terms of energy consumption.

Early attempts to optimize condensation-type clothes dryers were made by Kadoya et al. [76], focusing on the fan module. Their work led to a simplified system and reduced equipment weight and cost. This optimization approach was further refined by Kim et al. [77] using the Taguchi design of experiment (DOE) method to enhance fan performance and reduce the noise [78].

The main shortcoming of early-stage research was the absence of a strong theoretical foundation. These studies followed a similar routine, involving the measurement of key parameters, such as temperature and humidity indices, throughout the drying process while assessing their sensitivity to inlet conditions. Although they successfully optimized and predicted drying workflows, the absence of a comprehensive mathematical model limited the generalizability of their findings to other dryers.

On the other hand, the individual components of a tumble dryer, such as the fan/heater unit, rotating drum, and condenser, are widely used in many industrial applications, and consequently a substantial body of literature exists that investigates each of these elements separately [28,79–86]. While these studies offer valuable insights into individual components, the intricate nature of tumble dryer operation necessitates an integrated approach. The drying cycle, occurring within the drum, represents a crucial aspect of the condenser dryer. Ideally, examining the drum alone could provide essential parameters for evaluating the drying efficiency. However, the interconnected nature of the components within the tumble dryers prohibits such a modular, stand-alone approach. This complexity arises because the operating conditions of each module can significantly impact the performance of others.

For example, the gas flow rate in the fan channel is governed by the overall pressure drop across the remaining components of the system. A similar explanation exists for mass-transfer processes in the drum and condenser. As a result, evaluating the performance of any individual component requires consideration of the behavior of the entire dryer system. For this reason, many studies have employed a control-volume framework that includes all components and applies overall mass and energy balance equations to the system, such as the configuration illustrated in **Figure 8**, originally proposed by Deans for an open-loop vented dryer.

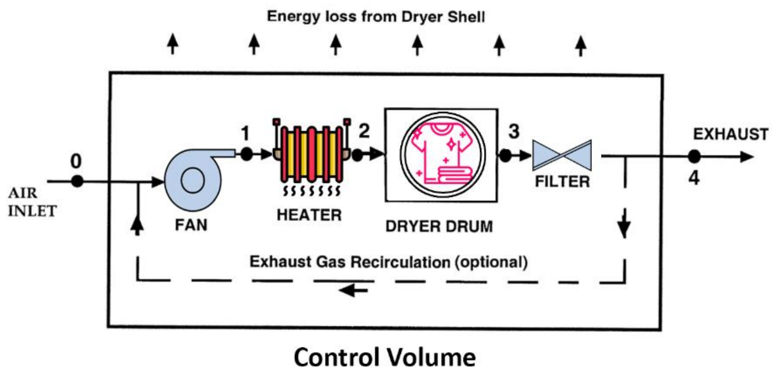

Figure 8. Box of the control volume around a semi-open-loop vented dryer [2].

This integrated approach has been the driving force behind the theoretical methodologies in the literature, allowing researchers to address mass and energy conservation for the system.

4.1. Lambert model

Understanding the precise relationship between machine parameters and the theoretical aspects of the drying cycle is crucial for advancing clothes-drying technologies [87]. The first significant step towards incorporating mathematical aspects into the study of drying machines has been made by Lambert et al. [1]. Their pioneering work aimed to develop a heat and mass transfer model for the drying process in textile tumble dryers by means of the Chilton-Colburn analogy (also known as the modified Reynolds analogy [88]), which relates heat and mass transfer phenomena [89]. This approach, widely employed in drying research across various domains, including porous media, semiconductors, food, and distillation, allowed them to estimate the mass evaporation rate in the drum using the following relationship [90–99]:

$$\dot{m}_{\mathrm{evap}} = kA(P_{\mathrm{t}} - P_{\mathrm{x}}) = kA(\omega_{in} - \omega_{out}) \ , \tag{2}$$

where k denotes the evaporation coefficients and A represents the surface area of the clothes. In most practical analyses, these two parameters are not treated separately; instead, their product kA is used as a single quantity, commonly referred to as the area–mass transfer coefficient. This parameter describes the mass transfer inside the drum and its importance will be explained in the following sections.

ω_{in} and ω_{out} are the absolute humidities at the inlet and outlet of the drum, respectively. P_{t} and P_{x} are the partial vapour pressure at the textile's surface and the drying air (bulk air), respectively. P_{t} is estimated as follows:

$$P_{\mathrm{t}}(x_{\mathrm{t}}, T_{\mathrm{t}}) = P_{\mathrm{sat}}(T_{\mathrm{t}})a(x_{\mathrm{t}}) \ , \tag{3}$$

where P_{sat} depends on temperature while the water activity, a, is determined by the moisture content of the medium to be dried. Although water activity is influenced in a complex manner by temperature and by the direction of the process (for example, drying versus wetting), the use of approximate empirical curves is generally sufficient for macroscopic analyses. The water activity and moisture relationship is commonly referred to as the sorption isotherm. A sorption-isotherm curve describes the relationship between the moisture content of a textile and the corresponding equilibrium relative humidity (i.e., water activity) at a fixed temperature. Namely, That is, at a fixed temperature, each value of relative humidity corresponds to a specific equilibrium moisture content of the material [100].Typically, an increase in water activity is associated with an increase in moisture content, although the relationship is strongly nonlinear [101]. These curves are determined experimentally, as they cannot be derived explicitly from analytical calculations. An example of a typical sorption-isotherm curve is presented in **Figure 9**. It should be noted that the paths followed during evaporation and condensation are generally different, meaning that the material does not necessarily follow the same curve in both processes. The exact shape of the sorption-isotherm depends on the properties of the textile material, and hysteresis, where the adsorption and desorption curves do not coincide, is a commonly observed feature in such systems [102].

In modeling fabric drying, it is usually sufficient to focus on desorption, namely the evaporation of moisture from the textile. One of the earliest systematic efforts to describe desorption rate for different fabrics was reported in [103] and it is still often cited as a starting point in this area. Using experimental data, Lambert proposed an empirical expression for estimating the activity coefficient [1]:

$$a = 1 - \frac{\beta M_{\mathrm{c}} + \delta}{1 + \delta^{\gamma M_{\mathrm{c}}}} \tag{4}$$

In this relation, M_{c} is the moisture content of the fabric, while β, δ and γ are material-dependent parameters. The fitted coefficients reported for different textiles are shown in **Figure 10**, comparing, for example, a highly porous material such as wool with lower-porosity fabrics such as nylon and cotton. A key implication of these results is that cotton tends to remain close to surface saturation during most of the drying cycle. Differences between fabrics become most relevant later in the process, once the overall moisture level has dropped and the desorption behaviour begins to influence evaporation more strongly.

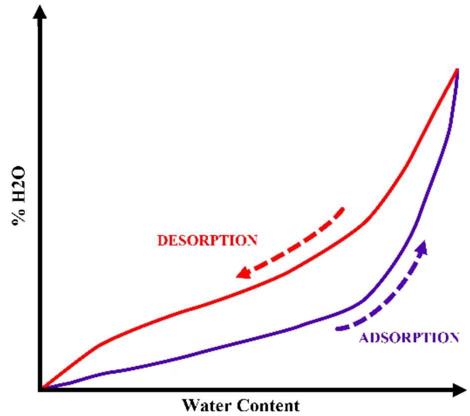

Figure 9. A typical moisture sorption isotherm curve.

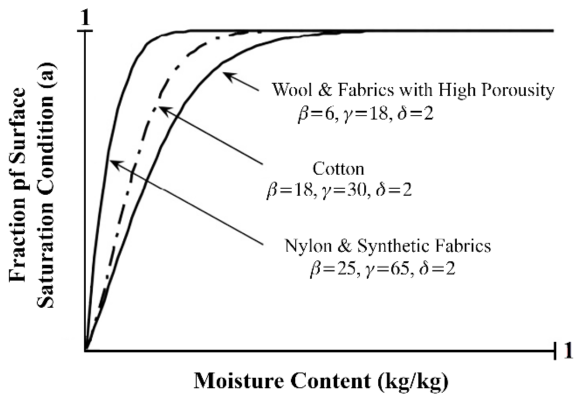

Figure 10. Equation 4 coefficients for different fabrics.

Subsequent studies introduced more detailed expressions for water activity during fabric drying. As an example, the model proposed by Yi incorporates both moisture content and textile temperature [61]:

$$(x, T_{cl}) = 1 - e^{\left(-\alpha . x(t) . h_{fg} / k_B . T_{cl}\right)} \tag{5}$$

where x denotes the vapor quality, h_{fg} is the latent heat of vaporization and k_B is the Boltzmann Constant.

Using Equation 2, Lambert also examined how the evaporation rate evolves over a full dryer run and suggested dividing the process into three broad stages. The cycle begins with a warm-up (transient) period. During this time, evaporation may already occur locally, but much of the heater input is spent bringing the load up to temperature. As a result, the overall moisture content changes little at first, while the evaporation rate rises from a low initial value (**Figure 11**).

In the next stage, once the load has warmed, the process typically enters a constant-rate period. Here the moisture content decreases steadily and most of the supplied energy is used directly for evaporation, as depicted in **Figure 11**. This regime is expected when the textile still contains enough moisture for the water activity to remain close to one over a sustained interval, which is common in tumble drying. Under these conditions, operating variables change only slowly.

As drying continues and the moisture content x_t becomes low, the water activity begins to fall below unity because the assumption of a freely evaporating water surface is no longer appropriate. The evaporation rate then drops and the energy that is no longer consumed by phase change increasingly goes into heating the fabrics and the drum. Part of the reduction in evaporation is offset by the rise in saturation pressure (P_{sat}) with temperature (Equation 3), but the system ultimately transitions into the falling-rate period. This stage is typically associated with higher exhaust-air temperatures and a decreasing rate of evaporation rate ($\dot{m}_{ev}$) [1].

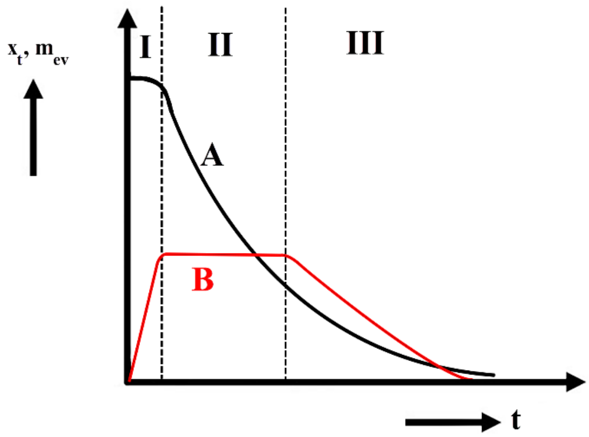

Figure 11. Schematic of the drying process: transient (I), constant rate (II) and falling rate (III) period. (A) Moisture contents in black line, x_t, versus time, *t*; (B) rate of evaporation in red line.

In Equation (2), the key remaining unknown is the area–mass transfer coefficient (*kA*). Because it represents a combination of several coupled mass-transfer mechanisms, there is no generally accepted model that predicts (*kA*) reliably across dryer designs and operating conditions. For this reason, literature treats it in different ways. One common approach is to estimate it indirectly using heat–mass transfer analogies [62]. In such treatments, a modified Lewis number is introduced to link the convective heat-transfer coefficient to the corresponding mass-transfer coefficient [35].

$$\mathrm{Le}' = \frac{h}{\lambda C_P} \quad (6)$$

Representative values of the convective heat-transfer coefficient, h, are reported in **Table 3**. Although the presence of evaporation might suggest using a phase-change heat-transfer coefficient, the dominant resistance is often associated with transfer between the moisture in the textile and the thin, near-saturated air layer at the fabric surface. This makes a forced-convection description more appropriate, and values in the range of $h = 20 \sim 100$ are frequently used. The wide spread of this range is not a minor detail: choosing h near the lower or upper bound can dramatically change the evaporation rate predictions. A further source of uncertainty is the effective surface area A in Equation (2), which is difficult to define for a tumbling, deforming textile load and is therefore handled using different assumptions across studies [62,104,105].

Table 3. Representative conductive heat transfer coefficient [106].

Process	**h(W/m²K)**
Natural Convection	
Air	1~10
Water	200~1000
Forced Convection	
Gas	20~ 250
Water	1000~1500
Phase Change	
Boiling	2500~3500
Condensation	5000~ 25000

Due to the complexities discussed above, several studies have adopted a simplified approach in which the area–mass transfer coefficient is assumed to be constant and determined from experimental measurements [2]. For example, Bengtsson et al. [107] used an experimentally determined value of 0.036 $kg/sBar$. Although this type of experimentally based constant can provide reasonable agreement with measurements under certain conditions, treating the coefficient as fixed throughout the process has clear limitations. In particular, the evaporation rate gradually decreases during the final stages of drying and therefore a single fixed value cannot accurately describe the rate over the entire drying cycle. Nevertheless, this simplification has frequently been used in simulations of heat pump tumble dryers, where the additional complexity introduced by modeling the heat pump loop often justifies adopting a constant transfer coefficient to keep the overall model tractable.

Back to the Lambert formulation, Equation (2), the model was applied to estimate the time evolution of the evaporation rate for nylon and cotton fabrics. The corresponding evaporation and moisture-content histories are shown in **Figure 12**. Both fabrics exhibit similar trends during the transient and constant-rate periods, while noticeable differences appear at the onset of the falling-rate stage, where the water activities of the materials deviate from unity and begin to differ significantly.

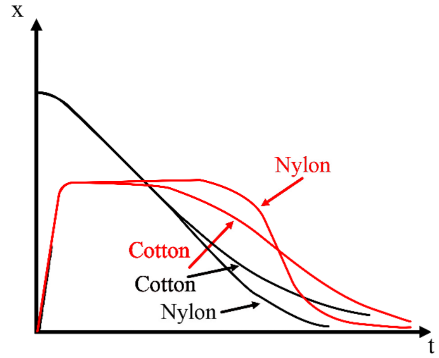

Figure 12. Schematic of the drying process for two types of fabrics. Black and red likes represent moisture content and evaporation rate, respectively.

Several extensions of Lambert's approach have also been proposed for modeling evaporation in tumble dryers, although many of these methods are mathematically involved and computationally expensive [108]. For instance, Ng and Deng developed a semi-empirical formulation applicable to the constant-rate and falling-rate periods of the drying cycle [26], while Haghi proposed a model based on rate equations describing moisture exchange between the fibers and the air within the textile pores [109]. Although such models can provide detailed local information, their complexity and high computational cost limit their suitability for optimization studies. In addition, they require extensive input data, including thermophysical properties and heat and mass transfer coefficients, which have received significant attention in the literature.

4.2. Deans model

Because of its relative simplicity and practical applicability, the Lambert formulation has been widely adopted and further developed in several studies to model the drying cycle [110–112]. Building on this framework, Deans proposed a mathematical model to evaluate dryer performance using overall mass and energy balance equations [2,113]. The model focuses primarily on the heat and mass transfer processes occurring within the drum and applies mass and energy balances to the air–vapour mixture at several nodes distributed throughout the dryer. The locations of these nodes, together with the corresponding airflow and energy-transfer paths, are illustrated in **Figure 8**. This formulation makes it possible to track energy inputs, losses, and air recirculation within the system, while also identifying components whose contributions are negligible and may therefore be omitted. The modular structure of the model further allows operating parameters—such as heater power—to vary during the cycle, which is particularly useful when assessing potential energy-saving strategies [2].

In practice, the drum is the central component in Deans' model, since its performance largely determines the mass and energy flows throughout the entire system. A key simplifying assumption is that the textiles, the contained moisture, and the drum walls share the same temperature. Because textile temperature is one of the most difficult variables to measure directly during operation [114], it is instead obtained from the energy balance in the drum, leading to the following relation [2]:

$$\frac{\mathrm{d}T_{\mathrm{clo}}}{\mathrm{d}t} = \frac{H_{\mathrm{in}} - H_{\mathrm{out}} - H_{\mathrm{evap}} - \dot{Q}_{\mathrm{loss}}}{\left(\dot{m}C_p\right)_{\mathrm{dryclo}} + \left(\dot{m}C_p\right)_{\mathrm{moist}} + \left(\dot{m}C_p\right)_{\mathrm{d}}}\ , \tag{7}$$

which can be rewritten as follows [2]:

$$\frac{T_{\mathrm{out}} - T_{\mathrm{clo}} - \left(\frac{H_{\mathrm{evap}} - \dot{Q}_{\mathrm{loss}}}{hA}\right)}{T_{\mathrm{in}} - T_{\mathrm{clo}} - \left(\frac{H_{\mathrm{evap}} - \dot{Q}_{\mathrm{loss}}}{hA}\right)} = \mathrm{e}^{-\left[\frac{hA}{\left(m_{\mathrm{a}}C_p\right)_{\mathrm{average}}}\right]}\ , \tag{8}$$

which equal to [115]:

$$T_{\mathrm{clo}+dt} = T_{\mathrm{clo}} + \left[\frac{\dot{m}_a(h_{\mathrm{in}} - h_{\mathrm{out}}) - \dot{Q}_{\mathrm{loss}} + \dot{m}_{\mathrm{evap}} h_{\mathrm{fg}}}{\dot{m}_{\mathrm{dryclo}} Cp_{\mathrm{dryclo}} + \dot{m}_{\mathrm{dryclo}} Cp_{moist} + \dot{m}_d Cp_d}\right] \Delta t \ . \tag{9}$$

Equation (9) is widely used to describe the time evolution of drum temperature and has been implemented in several subsequent studies [110–112]. The specific heat capacities, within the operating range, are considered constant values as their variation with temperature is relatively small. The enthalpy of vaporization, h_{evap}, depends on temperature, while the dry-air mass flow rate $\dot{m}_a$ entering the drum is usually determined experimentally.

Q_{loss} represents convective heat losses from the outer surfaces of the dryer to the surrounding air. This quantity depends on the machine geometry and on the temperature difference between the internal air mixture and the ambient environment, and it varies during the cycle as the operating temperatures change. Because the highest losses typically occur in the heater section where the air temperature is greatest, Deans approximated this term as a function of the heater-module temperature. Under this assumption, the heat-loss expression takes the following form [107]:

$$Q_{\mathrm{loss}} = \mathrm{Nu} \cdot \frac{\lambda_{\mathrm{a}}}{L_{th}} \cdot A_{ext}(T_{hater} - T_{amb}) \ , \tag{10}$$

where λ_{air} is the thermal conductivity of air, and L_{th} and A_{ext} denote the shell thickness and the external surface area of the dryer, respectively. The Nusselt number, defined as the ratio of convective to conductive heat transfer, is given by [106,116]:

$$\mathrm{Nu} = 0.13 \cdot (\mathrm{Gr} \cdot Pr)^{\frac{1}{3}} \quad 10^8 < \mathrm{Gr} \cdot Pr < 10^{12} \tag{11}$$

Gr and Pr are Grashof and Prandtl numbers, respectively, and are defined as follows:

$$\mathrm{Pr} = \frac{\nu}{\alpha} = \frac{\mathrm{Momentumdiffusivity}}{\mathrm{Thermaldiffusivity}} \tag{12}$$

$$\mathrm{Gr} = \frac{g\beta(T_{heater} - T_{ambient}){L_{th}}^3}{\nu^2} = \frac{\mathrm{BuoyancyForce}}{\mathrm{ViscousForce}} \tag{13}$$

where g and β are gravitational acceleration and the thermal expansion coefficient, respectively.

Dean proposed the following relation instead of that of Lambert (Equation (2)) for the evaporation rate:

$$\dot{m}_{\mathrm{evap}} = kA\left[a\omega_{\mathrm{surf}} - \frac{[\omega_{\mathrm{inlet}} + \omega_{\mathrm{exhaust}}]}{2}\right] \ , \tag{14}$$

and therefore:

$$\dot{m}_{\mathrm{a}}[\omega_{\mathrm{inlet}} - \omega_{\mathrm{exhaust}}] = kA\left[a\omega_{\mathrm{surf}} - \frac{[\omega_{\mathrm{inlet}} + \omega_{\mathrm{exhaust}}]}{2}\right] \tag{15}$$

For the sake of simplicity, some authors considered the humidity ratio of clothes equal to that of the inlet [83]:

$$\dot{m}_{\mathrm{a}}[\omega_{\mathrm{inlet}} - \omega_{\mathrm{exhaust}}] = kA\left[a\omega_{\mathrm{inlet}} - \frac{[\omega_{\mathrm{inlet}} + \omega_{\mathrm{exhaust}}]}{2}\right] \ , \tag{16}$$

where ω_{surf}, ω_{inlet} and ω_{exhaust} represent the humidity ratios of the saturated air at the textile surface and of the air at the drum inlet and outlet, respectively, while $\dot{m}_{\text{a}}$ denotes the dry-air mass flow rate at the inlet. The only unknown in Equation (15) is the outlet humidity ratio, $\omega_{exhaust}$, which can be determined as a function of time; once this quantity is known, the evaporation rate, $\dot{m}_{\text{evap}}$, can be calculated accordingly.

By solving the coupled mass- and energy-balance equations, Deans was able to predict the temporal evolution of the main operating variables in the dryer, as illustrated in **Figure 13**. The parameters associated with the drum are presented on the left-hand side of the figure. The relative humidity inside the drum (chart A) is predicted to remain close to 100% during most of the cycle, except at the beginning and end (corresponding to the transient and falling-rate stages). The predicted textile and outlet-air temperatures (charts B and C) exhibit similar trends, while the evolution of the moisture content (chart D) follows the general behaviour described earlier (**Figure 11**). Additional performance indicators for the entire control volume (**Figure 8**) are shown on the right-hand side.

He also carried out a numerical sensitivity study to evaluate how operating conditions influence drying time and energy performance. Based on the results, ambient humidity extends the drying process time, leading to increased energy consumption. In contrast, higher ambient temperature, greater airflow, and increased supplied power were found to reduce the drying time and improve overall efficiency. In this case, the input power represents the combined power consumption of the fan, the rotating drum, and the heater.

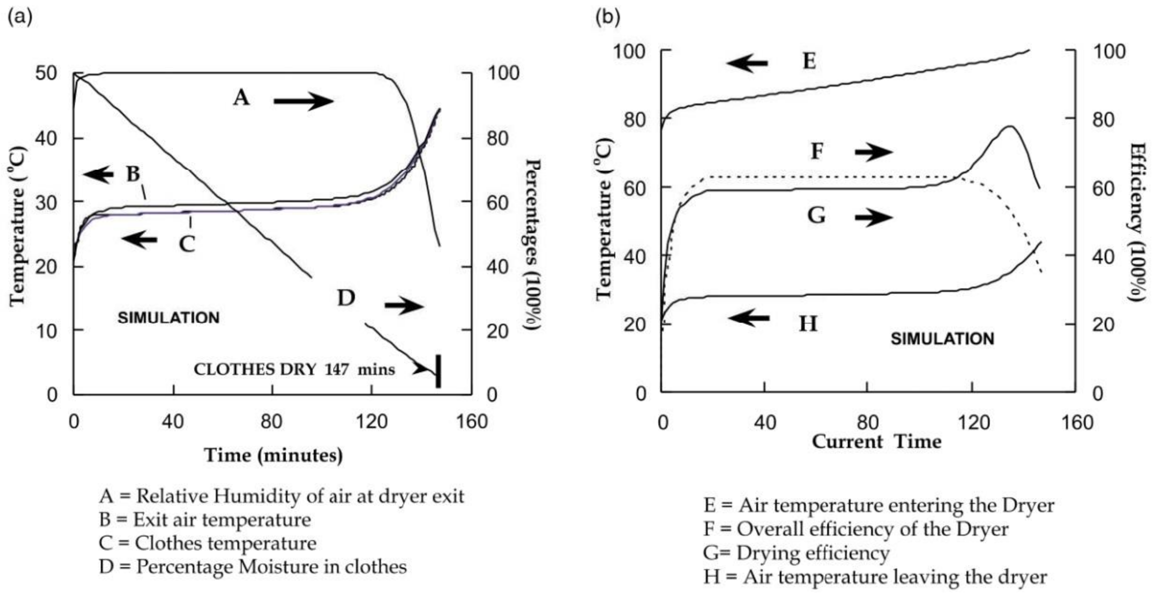

Figure 13. Results of numerical model of Deans [2] illustrate the time-dependent variation of fabric temperature, moisture content, and air conditions for a 4.16 kg cotton load with a 1.6 kW heater and a 0.020 kg/s air flow rate to demonstrate the high correlation between the simulation and experimental performance tests. (a) Time-dependent variation of relative humidity of air at the dryer exit, exit air temperature, clothes temperature, and percentage moisture in clothes; (b) Time-dependent variation of air temperature entering the dryer, overall efficiency of the dryer, drying efficiency, and air temperature leaving the dryer.

The numerical framework proposed by Deans provided a basis for many later studies aimed at modelling clothes-drying cycles [62,65,112]. Gluesenkamp adopted a similar modelling strategy to evaluate drying performance in subsequent work [114,117]. **Figure 14** illustrates the macroscopic mass representation together with the differential states of both the clothing load and the air–vapour mixture within the system. For a textile element inside the drum, the evolution of sensible and latent energy can be expressed as follows:

$$\dot{m}_a c_p dT = h\ dA(T_{\mathrm{surf}} - T) \tag{17}$$

$$\dot{m}_a h_{fg} d\omega = k\ dA(\omega_{\mathrm{surf}} - \omega) h_{fg} \tag{18}$$

where T_{surf} and ω_{surf} denote the temperature and humidity ratio at the textile surface, respectively, which are assumed to remain uniform throughout the drum. A and h_{fg} denote the effective wet surface area and the latent heat of evaporation of water, respectively. By assuming that the textile surface temperature remains uniform, the governing differential equations can be integrated over the entire fabric surface, resulting in Eqs. 19 and 20, which represent the overall heat and mass transfer rate [117].

$$T_{\mathrm{out}} = T_{\mathrm{surf}} - (T_{\mathrm{surf}} - T_{\mathrm{in}}) e^{-NTU} \tag{19}$$

$$\omega_{\mathrm{out}} = \omega_{\mathrm{surf}} - (\omega_{\mathrm{surf}} - \omega_{\mathrm{in}}) e^{-NTU} \tag{20}$$

where NTU is defined as the number of transfer units [118]:

$$TU = \frac{hA_t}{\dot{m}_a c_p}\ , \tag{21}$$

or as a general rule for the heat exchanger [106]:

$$\mathrm{NTU} = -\ln(1 - \varepsilon) \tag{22}$$

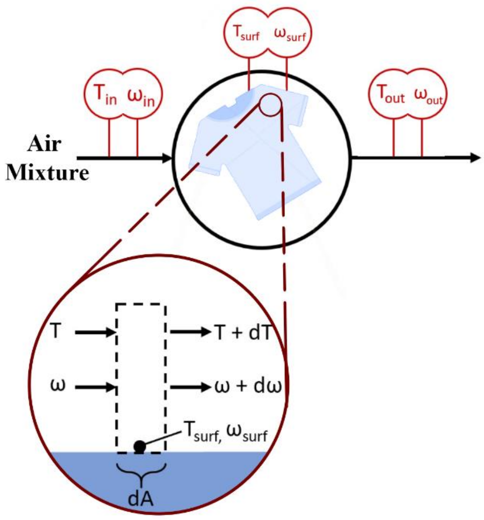

Figure 14. Macro-level (top) and differential view (bottom) of the heat and mass transfer process in a dryer drum, modeling the air/vapour mixture enthalpy changes and moisture evaporation.

By rewriting Equations (19) and (20), they could introduce two parameters, namely heat and moisture transfer effectiveness, could be introduced to address the efficiency of the drying cycle:

$$\varepsilon_{\mathrm{H}} = 1 - \frac{\mathrm{T_{surf}} - \mathrm{T_{out}}}{\mathrm{T_{surf}} - \mathrm{T_{in}}} \tag{23}$$

$$\varepsilon_{\mathrm{M}} = 1 - \frac{\omega_{\mathrm{surf}} - \omega_{\mathrm{out}}}{\omega_{\mathrm{surf}} - \omega_{\mathrm{in}}} \tag{24}$$

Indices in, out and $surf$ refer to the drum inlet, drum outlet, and textile surface regions. Air temperature and specific humidity at the inlet and outlet were obtained directly from sensor measurements. Since direct measurement of textile temperature and moisture content during operation is challenging, two simplifying assumptions were introduced.

First, the textile surface was assumed to remain saturated:

$$\omega_{\mathrm{surf}} = \omega_{\mathrm{surf,sat}} \tag{25}$$

This assumption makes it possible to express the surface humidity ratio as a function of surface temperature. By combining Equations (24) and (25), the following expression is obtained:

$$\varepsilon_{\mathrm{M}} = 1 - \frac{\omega_{\mathrm{surf,sat}} - \omega_{\mathrm{out}}}{\omega_{\mathrm{surf,sat}} - \omega_{\mathrm{in}}} \tag{26}$$

$\omega_{\mathrm{surf,sat}}$ depends on the saturated vapour pressure evaluated at the textile surface temperature, (i.e., $P_{w,sat} = f(T_{surf})$), as well as on the atmospheric pressure, P_a, [114]:

$$\omega_{\mathrm{surf,sat}} = \frac{0.622 P_{w,sat}|_{T_{\mathrm{surf}}}}{\left(P_a - P_{w,sat}|_{T_{\mathrm{surf}}}\right)} \tag{27}$$

Recall that Lewis number characterizes fluid flows when there is both convective heat and mass transfer:

$$\mathrm{Le} = \frac{\mathrm{Sc}}{\mathrm{Pr}} = \frac{\alpha}{D} = \frac{\mathrm{Thermaldiffusivity}}{\mathrm{Massdiffusivity}} \tag{28}$$

where D is the diffusion coefficient. Sc and Pr represent Schmidt and Prandtl numbers, respectively. By assuming equal effectiveness for heat and mass transfer, equivalent to adopting a Lewis number equal to unity, Equations (23) and (24) become equivalent.:

$$\varepsilon_{\mathrm{H}} = \varepsilon_{\mathrm{M}} \tag{29}$$

This reduction in the number of unknown variables enabled the drying efficiency to be estimated by solving Equations (23)–(29). The overall modeling framework is summarized in **Figure 15**.

Gluesenkamp evaluated drying effectiveness for several experimental trials using a dry textile load of 3 kg, as shown in **Figure 16**. The results indicate that increasing the residence time has only a limited effect on effectiveness, whereas higher airflow rates and inlet temperatures improve drying performance throughout the cycle. A dimensional analysis was subsequently introduced to obtain a regression-based expression for the evaporation rate, which is discussed in Section 4.4.

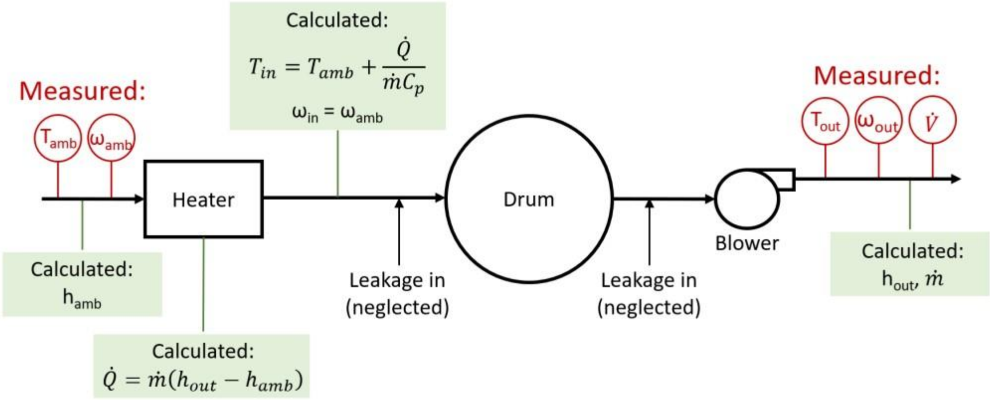

Figure 15. Process and instrumentation diagram of experimental evaluation in the work of Gluesenkamp et al. [114].

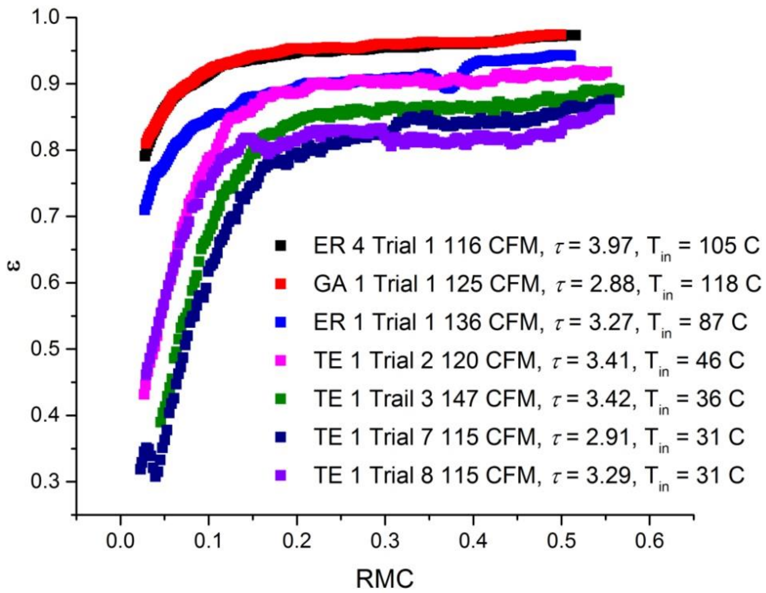

Figure 16. Effectiveness as a function of remaining moisture content for a 3.83 kg test cloth load [114]. The data illustrates the impact of varying drum residence times, fan flow rates, and drum inlet temperatures across three heating technologies: electric resistance, natural gas, and thermoelectric heat pump.

The original Deans model relied on a zero-dimensional formulation of the energy balance. Some later studies attempted to account for axial temperature variations within the drum by introducing a one-dimensional conductive heat-transfer model between textile layers [3]. However, these additional complexities did not lead to significant improvements in predictive accuracy compared with the simpler zero-dimensional approach.

More generally, many studies have adopted the same mass- and energy-balance philosophy introduced by Deans and Lambert to evaluate dryer performance, while differing mainly in the level of detail considered. For example, Conde investigated dryers equipped with heat-recovery heat exchangers, typically cross-flow air-to-air units used to preheat the inlet air stream [70].Huelsz et al. accounted for both radiative and convective heat losses from the dryer components in order to obtain more accurate predictions [119]. Unlike the Deans formulation, their model neglected air bypass while introducing a more detailed description of losses within the control volume. Jian and Zhao, on the other hand, investigated a dryer configuration equipped with a plate-fin heat exchanger in the condenser section and analyzed how variations in water flow rate influenced drying performance [113]. Lee et al. investigated dryer operation in the presence of a heat pump [115] and evaluated drying efficiency using the following relation [120], which has since been widely used in related work:

$$\eta_{dry} = \frac{T_{in}-T_{out}}{T_{\mathrm{in}}-T_{out}} = \frac{\omega_{out}-\omega_{in}}{\omega_{\mathrm{sat}}-\omega_{\mathrm{in}}} \tag{30}$$

Another commonly reported performance indicator is the specific moisture extraction rate (SMER) [86]:

$$\mathrm{SMER} = \frac{\dot{m}_{evap}}{PO_{tot}} \tag{31}$$

4.3. Yi model

A reliable estimate of the specific humidity at the textile surface, ω_{M}, in Equation (15) is important for describing the drying rate of the system. In many practical models, this quantity is simply taken to be equal to the saturation humidity ratio, $\omega_{\mathrm{M}} \approx \omega_{sat}$. Earlier work generally accounted for differences between fabric types by using sorption–isotherm diagrams (**Figure 9**); however, these relations are mainly obtained through empirical fitting of experimental data [121]. To move beyond purely empirical descriptions, Yi proposed an alternative formulation grounded in statistical thermodynamics, where Probability Density Functions (PDF) involving the Boltzmann constant were used to represent the evaporation process more physically [61].

$$m_{w,\mathrm{cl}}^{\mathrm{no-evap}}(\beta,\chi,T_{\mathrm{clo}}) = m_{w,\mathrm{clo}}^{\max} a(\beta,\chi,T_{\mathrm{clo}}) \tag{32}$$

$$a(\beta,\chi,T_{\mathrm{clo}}) = 1 - \exp\left(-\frac{\beta\chi Q_{\mathrm{LH}}}{k_B T_{\mathrm{clo}}}\right) \tag{33}$$

where $m_{w,\mathrm{clo}}^{\max}$ denotes the maximum moisture capacity of the textiles, $a(\beta,\chi,T_{\mathrm{clo}})$ is the activity coefficient, β characterizes the fabric type. The Q_{LH} is the latent heat of vaporization, while k_B is the Boltzmann constant [122]. Based on this formulation, the water activity coefficient can then be obtained through numerical evaluation.

The evaporation rate inside the drum was then estimated using a fluid-film analogy at the textile surface. Under this assumption, the moisture content of the adjacent air layer cannot exceed the saturation limit. Consequently, the specific humidity ω_{M} is constrained by the following inequality:

$$\begin{aligned} m_{\mathrm{air}}\omega_{\mathrm{M}} &= \gamma m_{w,\mathrm{clo}}^{\mathrm{no-evap}}(\beta,\chi,T_{\mathrm{clo}}) \\ &= \gamma m_{w,\mathrm{clo}}^{\max}(T_{\mathrm{clo}}) a(\beta,\chi,T_{\mathrm{clo}}) \\ &\geq m_{\mathrm{air}}\omega_{w,\mathrm{air}}^{\mathrm{sat}}(T_{\mathrm{clo}}) a(\beta,\chi,T) \end{aligned} \tag{34}$$

where γ represents a desorption weighting factor associated with the textile–air interface and takes a value smaller than unity. The obtained system of differential equations was solved in MATLAB. Model predictions were validated for two different textile types (**Figure 17**) and for varying load masses (**Figure 18**). The results show that synthetic and cotton fabrics experience comparable temperature ranges during drying, while the drying time increases approximately linearly with the load mass.

4.4. Dimensional analysis

Most of the previously discussed approaches rely on the Chilton–Colburn analogy to describe mass-transfer processes within the drum. Alternatively, some researchers have adopted dimensional-analysis techniques based on the Sherwood number to relate machine operating parameters to evaporation rate. One of the early contributions in this direction was presented by Bassily [123].

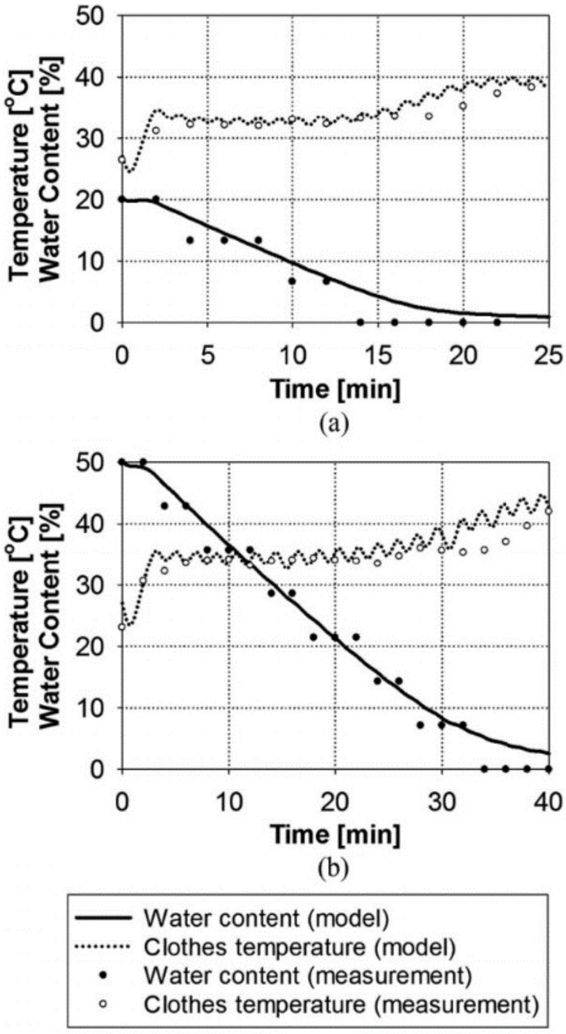

Figure 17. Comparison of the clothes temperature and water content between the simulation and the experiments for (**a**) synthetic fabrics and (**b**) cotton fabrics [61]. The synthetic fabric consists of 35% cotton and 65% polyester, while the cotton fabric is 100% cotton. The simulation (solid lines) and experimental data (data points) show the drying trajectory for varying mass under identical operating conditions.

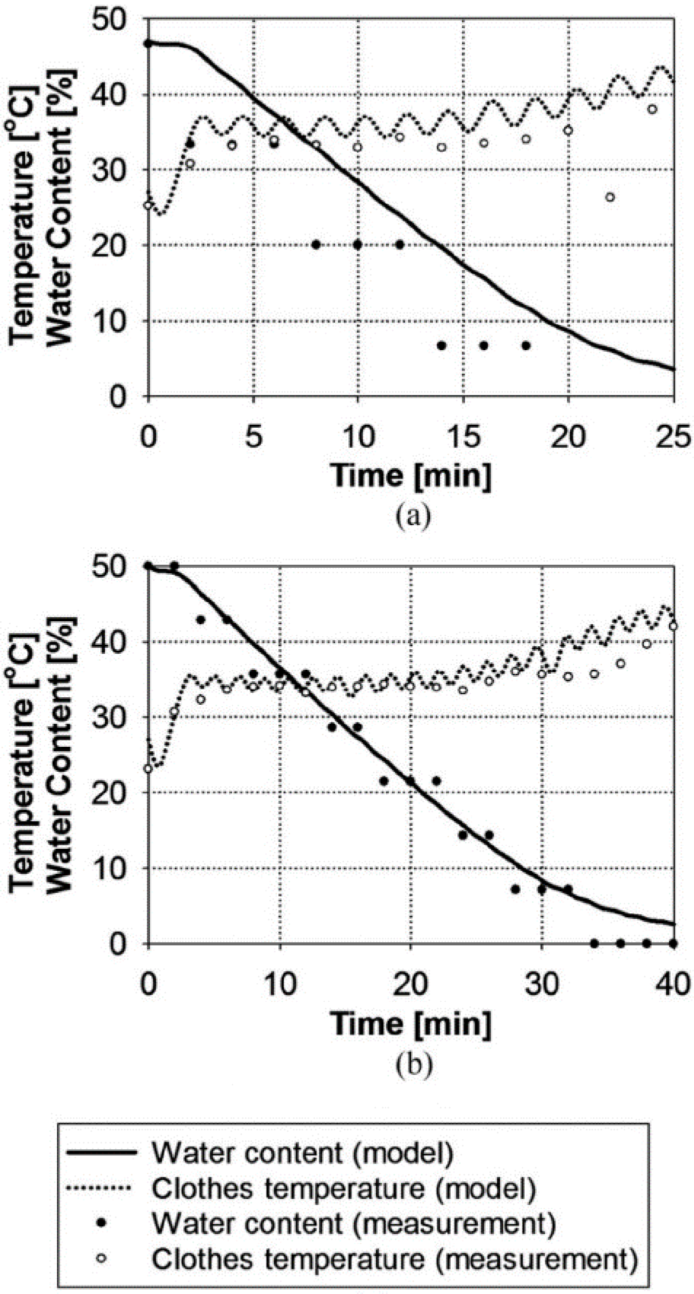

Figure 18. Comparison of the clothes temperature and the water content of different clothes loads: (**a**) 1.5 kg and (**b**) 2.8 kg [61]. The simulation (solid lines) and experimental data (data points) show the drying trajectory for varying mass under identical operating conditions.

The Sherwood number, (*Sh*) (often referred to as the mass-transfer analogue of the Nusselt number), represents the ratio between convective mass transfer and diffusive mass transport [124]:

$$\mathrm{Sh} = \frac{h_{evap}L}{D} = \frac{\text{Convectionmasstransfer}}{\text{Diffusionrate}} \tag{35}$$

where h_{evap} and L are the convective mass transfer coefficient and length scale, respectively.

Bassily proposed a dimensionless correlation for estimating the area-Sherwood number $\mathrm{Sh_a}$ (defined later) as a function of drum rotational speed $\mathrm{N_d}$, t, textile load mass, $\mathrm{M_t}$, Reynolds number, Re, Schmidt number, Sc, and Gukhman number, Gu. The Schmidt and Gukhman numbers are defined as follows [125,126]:

$$\mathrm{Sc} = \frac{\nu}{D} = \frac{\text{Momentumdiffusivity}}{\text{Diffusionrate}} \tag{36}$$

$$\mathrm{Gu} = \frac{T_g - T_{gw}}{T_g} \tag{37}$$

where T_g and T_{gw} are gas dry and wet bulb temperatures, respectively.

They found the following relation for the Sh_a using 32 experimental runs:

$$\mathrm{Sh}_a = 0.028 M_t^{0.58} N_d^{0.06} \mathrm{Gu}^{-1.38} \mathrm{Re}^{0.35} \mathrm{Sc}^{1.22} \tag{38}$$

Then the area-Sherwood number Sh_a can be used to estimate the area-mass transfer coefficient, kA, as follows [127]:

$$A = \frac{\mathrm{Sh}_a \times D}{d_d}\ , \tag{39}$$

where d_d is the drum diameter and D denotes the diffusion coefficient. The diffusion coefficient is a function of the instantaneous moisture content, $C(t)$:

$$D = -1.71778 \times 10^{-7} \left(\frac{C(t)}{1.2727}\right)^5 \times (-1387.462 - 1479.582 \times C(t) + 452.948 \times C(t)^2) \tag{40}$$

More recent studies have increasingly focused on correlating drying performance indicators directly with machine operating parameters [38,117]. For example, Novak et al. proposed regression relations linking drying time, evaporation rate, and the area–mass transfer coefficient to volumetric airflow rate, inlet air temperature, and relative humidity as follows:

$$t \quad = 39434 \times \dot{V}_{\mathrm{in}}^{-0.9065} T_{\mathrm{in}}^{-0.8338} \mathrm{RH}_{\mathrm{in}}^{0.1598} \tag{41}$$

$$\dot{m}_{\mathrm{evap}} \quad = 5.53 \times 10^{-7} \dot{V}_{\mathrm{in}}^{0.8305} T_{\mathrm{in}}^{0.8066} \mathrm{RH}_{\mathrm{in}}^{-0.1914} \tag{42}$$

$$kA \quad = 9.06 \times 10^{-8} \dot{V}_{\mathrm{in}}^{0.6824} T_{\mathrm{in}}^{-0.5561} \mathrm{RH}_{\mathrm{in}}^{-0.0293} \tag{43}$$

Gluesenkamp developed a correlation to predict the effectiveness of coupled heat and mass transfer phenomenon inside the drum. In this formulation, effectiveness depends on five main variables: the textile load mass m_c, the moisture content of the textiles m_w, the air mass within the drum m_a, the air inlet flow rate $\dot{m}_a$ and the falling time t, defined as the time required for a textile item to fall from the top to the bottom of the rotating drum:

$$= f(m_{clo}, m_w, m_a, \dot{m}_a, t) \tag{44}$$

By means of Buckingham π-theorem they could find the following dimensionless parameters:

$$\begin{aligned} \pi_1 &= \varepsilon \\ \pi_2 &= \frac{\dot{m}_a t}{m_a} \\ \pi_3 &= \frac{m_{clo}}{m_a} \\ \pi_4 &= \frac{m_w}{m_a} \end{aligned} \tag{45}$$

They took the first-order polynomial for π_2 and π_3 where a fourth-order polynomial is considered for π_4:

$$\pi_1 = a + b_1\pi_2 + c_1\pi_3 + d_1\pi_4 + d_2\pi_4^2 + d_3\pi_4^3 + d_4\pi_4^4 \tag{46}$$

A series of experiments was conducted to determine the coefficients appearing in Equation 46 for two standardized textile loads, namely HLD-1-1992, comprising cotton-like items such as sheets, tablecloths, bath towels, long-sleeve shirts, T-shirts, pillowcases, shorts, washcloths, and handkerchiefs [128] and HLD-1-2009, which includes 100% cotton sheets, pillowcases, and towels [129]. The resulting coefficient values are summarized in **Table 4**.

Table 4. Coefficients in Equation (46) [117].

Coefficient	AHAM 2009	AHAM 1992
a	0.677584	0.354049
b_1	−4.456546	−2.11532
c_1	0.015385	0.00212
d_1	0.290916	0.403633
d_2	−0.071735	−0.087495
d_3	0.007304	0.008034
d_4	−0.000249	−0.000252

So far, limited attention has been given to sensitivity analysis of dryer input parameters, and consequently there is no clear agreement which variables should be treated as independent in regression-based models. For instance, Gluesenkamp's formulation did not include drum rotational speed or air temperature among the governing parameters [117].

Moreover, although regression correlations are attractive because they can be implemented quickly without solving differential equations, the validity of the correlations holds only for the reference machine. In other words, such correlations cannot be generalized for other dryer configurations. In this context, Rasti and Jeong compared the regression models proposed by Bassily, Gluesenkamp, and Novak [127]. Their results showed that the Gluesenkamp and Novak formulations were able to reproduce the evaporation rate for low and medium textile loads, respectively (**Figure 19**). However, none of the models successfully captured the drying rate at higher loads

(9 kg), and the Bassily model failed to reproduce the observed trends for the tested machine under all conditions.

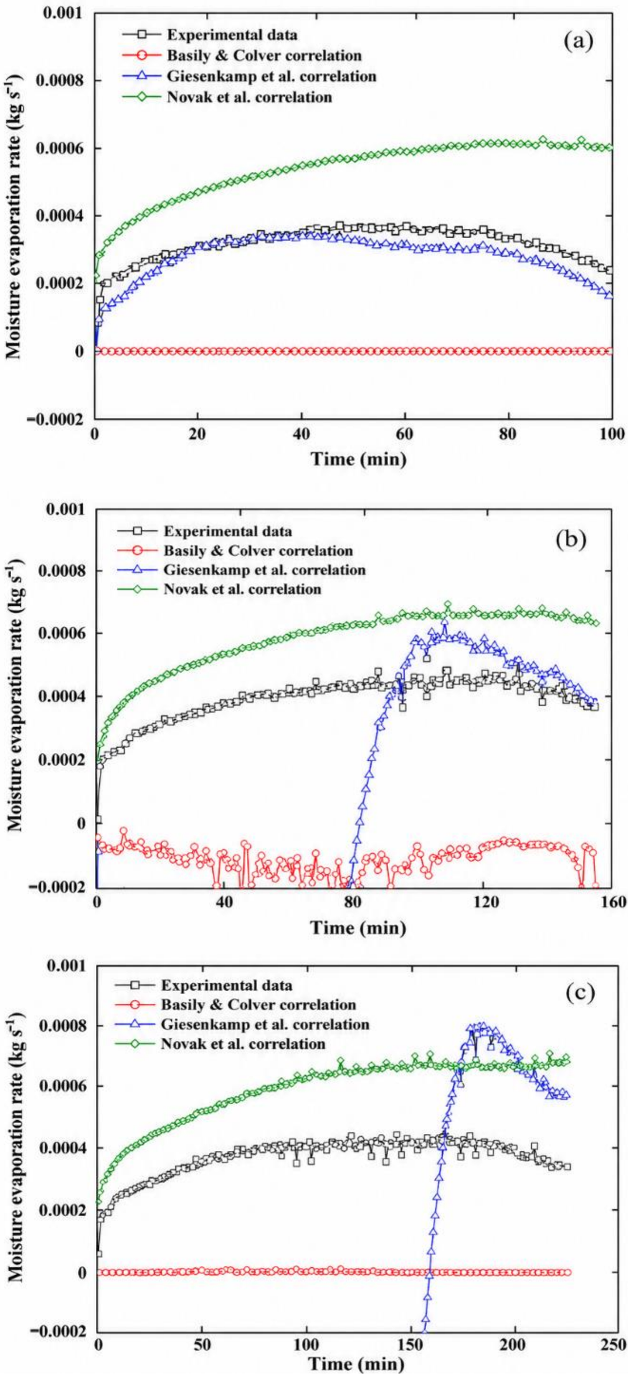

Figure 19. Comparison of the measured and predicted moisture evaporation rates using different correlations for (**a**) 3 kg load, (**b**) 6 kg load, and (**c**) 9 kg load [127]. All experiments were conducted using a heat pump tumble dryer starting at an initial moisture content of 60%. The test loads consisted of standard textiles (sheets, pillows, and towels) as specified in the experimental validation. Results indicate that while the Novak et al. correlation generally provided lower average absolute deviations, none of the models maintained high accuracy across the full range of load masses, particularly as the load increased toward 9 kg.

4.5. Kinematic models

Recent advances in measurement techniques have opened new research directions in tumble dryer studies. Several works have attempted to link evaporation thermodynamics with the kinematic of clothes inside the rotating drum. Modern optical diagnostics and high-speed imaging tools, such as Positron Emission Particle Tracking (PEPT), enable detailed visualization of airflow patterns and textile motion, allowing fabrics to be tracked throughout the drying process. Then, with the aid of image processing techniques, mainly Convolutional Neural Networks, the occupied area of the fabric along with the motion path is tracked in the drum through time. The cross-section of the drum is divided into four quadrants, as shown in **Figure 20**, for precise statistical analysis. Afterward, the center of gravity of the clothing is determined, with which they quantified the velocity profiles and residence time distribution to characterize the dynamics of cotton textiles.

Yu et al. utilized this methodology to assess SMER and drying uniformity index, known as evenness of drying [130]. They applied Equation (31) for SMER estimation. As for the drying uniformity, this procedure has been implemented:

- The weight of each individual piece, k, is measured after conditioning and drying. The final moisture content for each individual item k in the test load is:

$$\mu_{fk} = \frac{W_{fk} - W_{0k}}{W_{0k}} \times 100\% \tag{47}$$

where μ_{fk}, W_{fk} and W_{0k} are the final moisture content, final mass and the mass of the conditioned test load of the piece k, respectively.

- In the next step, one can calculate the average final moisture content of all the individual pieces in the test load, $\mu_{f_{avg}}$, as follows:

$$\mu_{f_{avg}} = \frac{1}{N} \sum_{k=1}^{N} \mu_{fk} \tag{48}$$

where N is the total number of load pieces.

- Evenness of drying is another definition for the standard deviation of the final moisture content of the pieces, which can be defined as:

$$s_w = \sqrt{\frac{1}{N} \sum_{k=1}^{N} \left(\mu_{fk} - \mu_{f_{avg}}\right)^2} \tag{49}$$

where s_w is the evenness of drying. A higher value of evenness of drying is an unfavourable condition in which more uneven drying can be found.

Finally, they reported SMER as follows:

$$\text{SMER} = -4.1 - 0.1x_1 + 0.02x_2 + 0.69x_3\ , \tag{50}$$

where x_1 and x_2 are the ratio of the total motion area of the tracer and the fabric spread area, respectively, and x_3 is the distance between the drum center and tracer fabric center. Similar studies have been done by [131–133].

This technique is also considered to be machine-specific. As there are only a few research studies relating to this technique, it is hard to assess it correctly compared to other methods.

Table 5 summarises the modeling categories reviewed, comparing them in terms of physical basis, accuracy, complexity, applicable conditions, and main limitations.

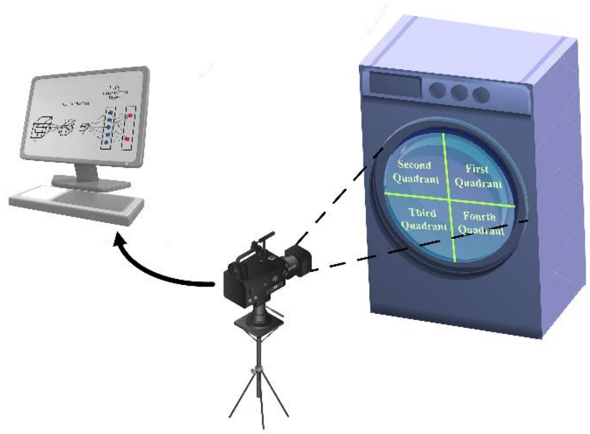

Figure 20. Schematic of the video capturing and processing system [132,133].

Table 5. Summary comparison of modeling approaches for evaporation-rate prediction and heat and mass transfer analysis in domestic tumble dryers.

Approach	Main principle	Accuracy	Complexity	Applicable conditions	Main limitations
Lumped energy-balance models	Overall mass and energy balances across drum and air loop	Moderate for global variables	Low to moderate	System-level analysis of vented, condenser, or heat-pump dryers	Assumes spatially uniform air/textile states; requires calibrated parameters
Chilton–Colburn-based models	Heat–mass transfer analogy with area–mass transfer coefficient kA	Moderate when calibrated	Moderate	Evaporation-rate estimation during transient and constant-rate drying periods	Sensitive to kA, textile area, water activity, and surface saturation assumptions
Constant evaporation-rate models	Fixed evaporation rate imposed during simulation	Low except over limited intervals	Low	Simplified heat-pump dryer simulations where refrigerant-cycle behaviour is the main focus	Cannot capture warm-up or falling-rate periods; poor generality
Dimensional / regression correlations	Empirical correlations using airflow, load mass, temperature, humidity, or drum speed	Good only within calibration range	Low	Rapid prediction for a specific machine and operating range	Machine-specific; weak extrapolation to new dryer geometries or higher loads
Physics-based desorption models	Fabric moisture activity and desorption behaviour included explicitly	Potentially high	High	Studies requiring textile-dependent evaporation prediction	Requires material properties, sorption data, and numerical solution of coupled equations
Kinematic / image-processing models	Fabric motion and exposure area obtained from imaging or particle tracking	Useful for motion-related drying analysis	High	Research on fabric motion, drying uniformity, and textile damage assessment	Requires optical access, image processing, and machine-specific calibration

5. Classification and applicability of evaporation-rate estimation methods

The approaches discussed above represent a substantial portion of the existing literature, most of which focuses on predicting dryer operation and performance. The objective of both numerical and experimental methodologies is to accurately estimate the evaporation rate. Once this quantity is known, the performance of the drying system can be evaluated. Among these, the specific moisture extraction rate, SMER, and drying time are particularly important. Additional aspects, such as drying uniformity, can also be related to evaporation rate [133–135], and the drying rate has been shown to influence textile wrinkling during the cycle [136].

In general, four main approaches for predicting evaporation rate can be identified in the literature. The following sections describe these methods in detail.

5.1. Direct method

Direct measurement of the weight of the components in the drum has also been considered as a possible way to estimate evaporation rate during drying. In practice, however, this approach is challenging because the rotating drum continuously subjects the textiles to centrifugal and Coriolis forces, which introduce strong oscillations in the measured signal. As a result, only a limited number of studies have adopted this method [137]. Higgins et al., for example, used a platform scale with a sampling interval of 1 s to monitor the drum contents during operation. The resulting evolution of moisture content is presented in **Figure 21**. Although the measurements exhibit considerable noise, useful information can still be obtained after applying filtering and averaging procedures.

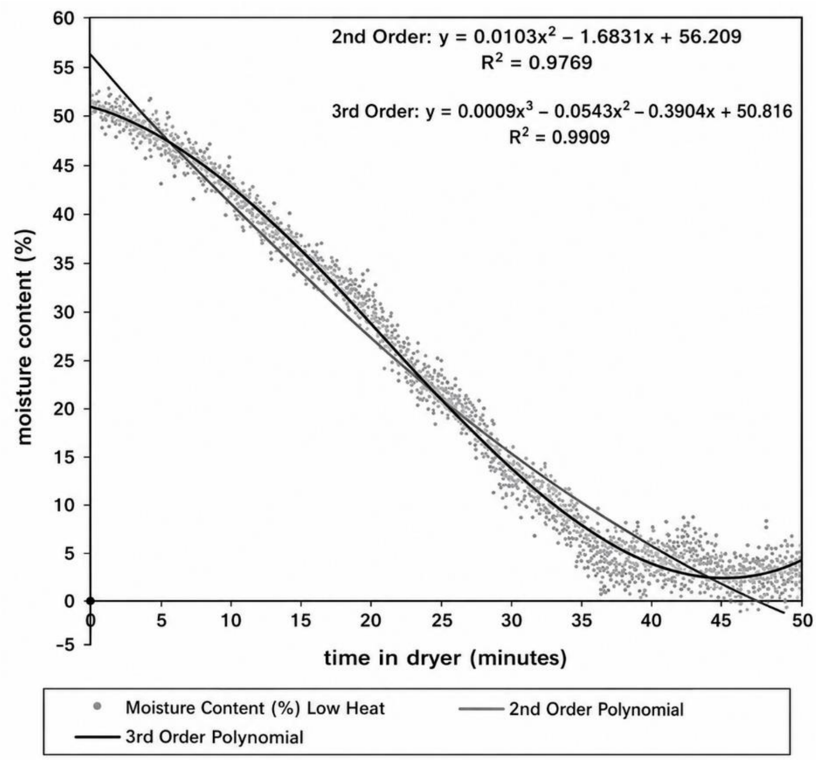

Figure 21. Change in moisture content during tumble-drying at low-temperature setting [137]. The drying loads were standardized at 2.7 kg with ~50% moisture content consisted of four woven cotton specimens, four knitted cotton specimens, and woven ballast.

5.2. Constant rate

Another simplification occasionally reported in the literature is the assumption of a constant evaporation rate throughout the drying cycle [138]. We et al., for instance, adopted a fixed value of 3.5 $\frac{kg}{h}$ in their numerical simulations [139].

The changes in temperature and moisture content in the drum have a non-linear trend through time. For instance, the typical evolution of the clothes temperature and moisture over time are depicted in **Figures 22** and **23**. Implementation of the so-called constant rate for evaporation may cause errors in the estimation of the start (transient) and final (falling rate) stages of the drying.

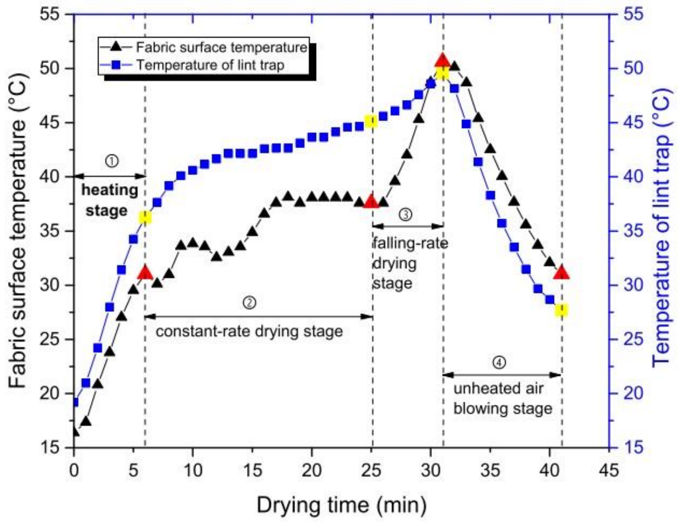

Figure 22. The changes of drum temperature during the drying process [131]. The experiment utilizes Haier GDZ10-977 dryer with a 3000 W heater and a rotating drum speed of 47 ±3 rpm to process six pieces of 80 × 80 cm^2 fabric.

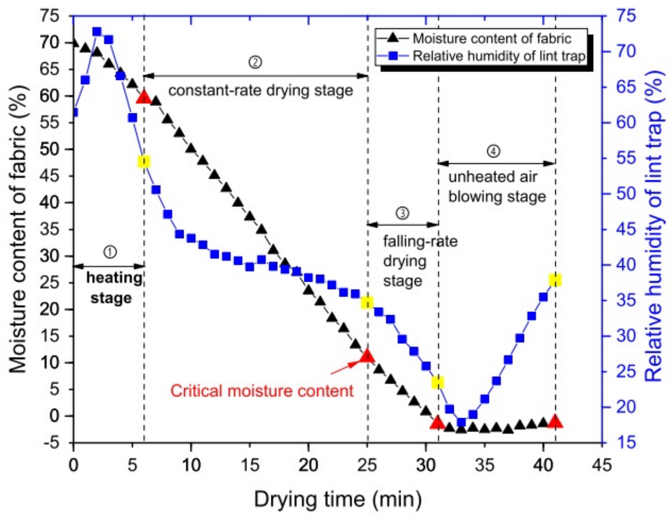

Figure 23. The changes of moisture during the drying process [131]. The experiment utilizes Haier GDZ10-977 dryer with a 3000 W heater and a rotating drum speed of 47 ±3 rpm to process six pieces of 80 × 80 cm^2 fabric.

As mentioned before, this assumption has mainly appeared in studies involving heat-pump dryers, where the main objective is often to analyze the performance of the heat-pump system rather than the drying rate itself. Because modelling the heat-pump cycle already introduces substantial complexity, adopting a constant evaporation rate is acceptable. For condenser tumble dryers, however, such a simplification is generally not appropriate.

5.3. Chilton-colburn analogy

As discussed in Section 4.1, Lambert's formulation expresses the evaporation rate using Equation (2), where kA can be treated as constant and estimated either through experimental regression or Sherwood-number analogies. **Figure 24** summarizes the main approaches used in the literature to estimate evaporation rate together with the associated performance indicators, while **Table 6** lists representative methodologies adopted in recent studies.

Figure 24. Methods for evaluating the evaporation rate of the tumble dryer.

Table 6. List of employed methodologies for evaporation rate in recent studies.

Researcher	Year	Model
Lee et al. [115]	2019	Chilton-Colburn
Huang et al. [62]	2019	Chilton-Colburn
Sian and Wang [140]	2019	Chilton-Colburn
El Fil and Garimella [141]	2021	Chilton-Colburn
Cranston et al. [142]	2019	Constant Rate
Novak et al. [38]	2019	Regression Model
Yu et al. [130]	2021	Image Processing
Zaman et al. [143]	2021	Image Processing
Yu et al. [69]	2023	Image Processing

6. Current situation and future

Recent research on tumble dryers has gradually shifted from simple performance evaluation to physically informed modeling, energy optimization, and sensor-based control. Heat-pump dryers have attracted particular attention because they can recover a portion of the thermal energy in the drying-air loop—but this benefit comes at the cost of increased modeling complexity, since the refrigerant cycle and the moist-air drying loop are now coupled. As a result, many studies still rely on simplified evaporation-rate expressions or calibrated transfer coefficients that do not fully capture this interaction.

Several research gaps remain unresolved. The area–mass transfer coefficient is routinely treated as constant, even though it is influenced by textile motion, load distribution, airflow rate, moisture content, fabric type, and drying stage. Many regression correlations are tuned to a specific machine and cannot be reliably transferred to different drum geometries, load sizes, or dryer configurations. The relationship between fabric kinematics and evaporation rate is still not adequately integrated into system-level models, and uncertainty quantification is rarely considered despite the fact that model predictions are highly sensitive to assumptions about effective surface area, textile temperature, water activity, and heat losses. Finally, the conditions under which models developed for vented, condenser, or heat-pump dryers remain valid are not always clearly stated, limiting how safely they can be reused.

Addressing these gaps points toward hybrid modeling strategies that combine the computational efficiency of lumped energy-balance frameworks with variable transfer coefficients, fabric-motion descriptors, and targeted experimental calibration. Sensor streams from temperature, humidity, and load-mass measurements and potentially from imaging systems, building on the kinematic approaches discussed in Section 4 could be used to update evaporation-rate models dynamically during a drying cycle. Alongside this, uncertainty-aware modeling and validation across different dryer types, textile loads, and operating conditions are needed before these models can be trusted for robust engineering design. Together, such developments would make dryer models genuinely useful for control optimisation, drying-time prediction, SMER improvement, fabric-care assessment, and energy-efficient appliance development.

7. Conclusion

Tumble dryers have become widely used household appliances because they provide a convenient and controlled method for drying textiles. This review examined mathematical approaches for modeling heat and mass transfer in domestic tumble dryers, with particular attention to evaporation-rate prediction as a key parameter governing drying time, efficiency, effectiveness, and specific moisture extraction rate (SMER).

The reviewed studies show that early and widely used models, particularly the Lambert and Deans formulations, established the basis for system-level dryer modeling through the Chilton–Colburn analogy and lumped mass and energy balances. These approaches remain useful because of their relative simplicity and practical applicability. However, their accuracy depends strongly on assumptions such as uniform textile temperature, saturated fabric surfaces, and calibrated or constant area–mass transfer coefficients. These assumptions are most acceptable during limited operating intervals but become less reliable during the warm-up and falling-rate stages, for mixed textile loads, or when models are transferred to different dryer configurations.

Subsequent developments, including the models of Gluesenkamp and Yi, dimensional-analysis methods, regression correlations, and kinematic/image-processing approaches, have improved the description of specific aspects of the drying process. Physics-based desorption models can better represent textile-dependent moisture behaviour, while regression correlations and dimensional models provide rapid prediction within calibrated operating ranges. Kinematic and image-processing methods are especially valuable when drying uniformity, fabric motion, and textile exposure area are of interest. Nevertheless, many of these approaches remain machine-specific, require extensive experimental data, or have limited extrapolation capability.

From an engineering standpoint, lumped energy-balance models are recommended for preliminary system-level design, control-oriented simulations, and comparison of dryer configurations. Chilton–Colburn-based models are suitable when evaporation-rate prediction is required, but only after calibration of the area–mass transfer coefficient for the target dryer, textile load, and operating range. Constant evaporation-rate or constant kA assumptions should be restricted to narrow operating windows or simplified heat-pump cycle studies, and should not be applied across a full drying cycle without validation. For heat-pump dryers, evaporation models should be coupled with refrigerant-cycle dynamics rather than treated as independent drum-level correlations.

Overall, the review indicates that no single modeling strategy is universally applicable to all dryer types, load conditions, and drying stages. Future dryer models should therefore incorporate variable transfer coefficients, explicitly stated dryer-type-specific boundaries, fabric-motion effects, and formal uncertainty analysis. Such developments are necessary to improve predictive reliability and support the design, optimisation, and control of more energy-efficient tumble dryers.

Author contributions: Conceptualization and methodology and investigation, Sajad Salavatidezfouli; writing—original draft preparation and review and editing, Sajad Salavatidezfouli, Giovanni Stabile, Arash Hajisharifi, Michele Girfoglio; project administration, Gianluigi Rozza. All authors have read and agreed to the published version of the manuscript.

Conflict of interest: The authors declare no conflict of interest.

References

1. Lambert AJD, Spruit FPM, Claus J. Modelling as a tool for evaluating the effects of energy-saving measures. Case study: A tumbler drier. Applied Energy. 1991; 38(1): 33–47. doi: 10.1016/0306-2619(91)90089-9
2. Deans J. The modelling of a domestic tumbler dryer. Applied Thermal Engineering. 2001; 21(9): 977–990. doi: 10.1016/S1359-4311(00)00096-9
3. Wei Y, Hua J, Ding X. A mathematical model for simulating heat and moisture transfer within porous cotton fabric drying inside the domestic air-vented drum dryer. The Journal of The Textile Institute. 2017; 108(6): 1074–1084. doi: 10.1080/00405000.2016.1219473
4. Menon A, Stojceska V, Tassou SA. A systematic review on the recent advances of the energy efficiency improvements in non-conventional food drying technologies. Trends Food Sci Technol. 2020; 100: 67–76. doi: 10.1016/j.tifs.2020.03.041
5. Acar C, Dincer I, Mujumdar A. A comprehensive review of recent advances in renewable-based drying technologies for a sustainable future. Drying Technology. 2022; 40(6): 1029–1050. doi: 10.1080/07373937.2020.1849270
6. Miraei Ashtiani SH, Rafiee M, Mohebi Morad M, Martynenko A. Cold plasma pretreatment improves the quality and nutritional value of ultrasound-assisted convective drying: The case of goldenberry. Drying Technology. 2022; 40(8): 1639–1657. doi: 10.1080/07373937.2021.1885059
7. Ksit B, Szymczak-Graczyk A, Nazarewicz B. Diagnostics and renovation of moisture affected historic buildings. Civil and Environmental Engineering Reports. 2022; 32(1). doi: 10.2478/ceer-2022-0001
8. Gopinath GR, Muthuvel S, Muthukannan M, et al. Design, development, and performance testing of thermal energy storage based solar dryer system for seeded grapes. Sustainable Energy Technologies and Assessments. 2022; 51: 101923. doi: 10.1016/j.seta.2021.101923

9. Stawreberg L, Berghel J, Renström R. Energy losses by air leakage in condensing tumble dryers. Applied Thermal Engineering. 2012; 37: 373–379. doi: 10.1016/j.applthermaleng.2011.11.050
10. Zahed AH, Zhu JX, Grace JR. Modelling and simulation of batch and continuous fluidized bed dryers. Drying Technology. 1995; 13: 1–28. doi: 10.1080/07373939508916938
11. Khaldi S, Korti AIN, Abboudi S. Improving the airflow distribution within an indirect solar dryer by modifications based on computational fluid dynamics. International Journal of Air-Conditioning and Refrigeration. 2017; 25(03): 1750022. doi: 10.1142/S2010132517500228
12. Alishah A, Kiamahalleh MV, Yousefi F, Emami A, Kiamahalleh MV. Solar-assisted heat pump drying of coriander: an experimental investigation. International Journal of Air-Conditioning and Refrigeration. 2018; 26(04): 1850037. doi: 10.1142/S2010132518500375
13. Oueslati H, Mabrouk S Ben, Mami A. Thermal Modeling of Solar Dryer—Numerical Simulation, Analysis and Performance Evaluation. International Journal of Air-Conditioning and Refrigeration. 2018; 26(04): 1850032. doi: 10.1142/S2010132518500326
14. Salhi M, Chaatouf D, Raillani B, et al. Numerical Analysis of the Dynamic and Thermal Behavior of an Indirect Solar Dryer: Effect of the Outlet. International Journal of Air-Conditioning and Refrigeration. 2021; 29(01): 2150001. doi: 10.1142/S2010132521500016
15. Wang D, Cao X, Li X, Li Y, Wang X. Experimental investigation of a part air dehumidification cascade-like heat pump drying system. International Journal of Refrigeration. 2021; 131: 235–243. doi: 10.1016/j.ijrefrig.2021.07.025
16. Azil A, Touati K, Sebaibi N, et al. Monitoring of drying kinetics evolution and hygrothermal properties of new earth-based materials using climatic chamber simulation. Case Studies in Construction Materials. 2023; 18. doi: 10.1016/j.cscm.2022.e01758
17. Bhatsada A, Patumsawad S, Itsarathorn T, et al. Improvement of energy recovery potential of wet-refuse-derived fuel through bio-drying process. J Mater Cycles Waste Manag. 2023; 25(2): 637–649. doi: 10.1007/s10163-022-01556-w
18. Lamrani B, Bekkioui N, Simo-Tagne M, Ndukwu MC. Recent progress in solar wood drying: An updated review. Drying Technology. 2023; 41(5): 605–627. doi: 10.1080/07373937.2022.2102037
19. Çetin N, Ciftci B, Kara K, Kaplan M. Effects of gradually increasing drying temperatures on energy aspects, fatty acids, chemical composition, and in vitro ruminal fermentation of acorn. Environmental Science and Pollution Research. 2023; 30(8): 19749–19765. doi: 10.1007/s11356-022-23511-2
20. Yang DL, Liu RK, Wei Y, Sun Q, Wang JX. Micro-sized nanoaggregates: Spray-drying-assisted fabrication and applications. Particuology. 2024; 85: 22–48. doi: 10.1016/j.partic.2023.05.001
21. Farinha S, Sá J V, Lino PR, et al. Spray freeze drying of biologics: a review and applications for inhalation delivery. Pharmaceutical Research. 2023; 40(5): 1115–1140. doi: 10.1007/s11095-023-03484-2
22. Kudra T. Energy aspects in drying. Drying Technology. 2004; 22(5): 917–932. doi: 10.1081/DRT-120038572
23. Kemp IC. Fundamentals of energy analysis of dryers. Modern drying technology. 2011; 4: 1–46. doi: 10.1002/9783527631720.ch1
24. Defraeye T. Advanced computational modelling for drying processes-A review. Applied Energy. 2014; 131: 323–344. doi: 10.1016/j.apenergy.2014.06.027
25. Kerkhof PJ, Coumans WJ. Drying: a fascinating unit operation. Chemical Engineering Journal. 2002; 1(86): 1–2. doi: 10.1016/S1385-8947(01)00246-5
26. Ng AB, Deng S. A new termination control method for a clothes drying process in a clothes dryer. Applied Energy. 2008; 85(9): 818–829. doi: 10.1016/j.apenergy.2008.01.002
27. Minea V. Overview of heat-pump-assisted drying systems, part I: Integration, control complexity, and applicability of new innovative concepts. Drying Technology. 2015; 33(5): 515–526. doi: 10.1080/07373937.2014.985794
28. Mensah K, Choi JM. Energy consumption and stability investigation of constant temperature and humidity test chamber. International Journal of Air-Conditioning and Refrigeration. 2017; 25(01): 1750010. doi: 10.1142/S2010132517500101
29. Gatarić P, Širok B, Hočevar M, Novak L. Influence of load mass, drum speed and load composition on evenness of drying in a heat pump tumble dryer. Drying Technology. 2021; 1–13. doi: 10.1080/07373937.2021.1925298
30. Chung YM, Chung BJ, Kim DS. Analysis of Residential Electricity Usage Characteristics and the Effects of Shifting Home Appliance Usage Time under a Time-of-Use Rate Plan. Energies (Basel). 2023; 16(18): 6602. doi: 10.3390/en16186602

31. Maya-Drysdale L, Iversen NH, Gydensen A, Skov Hanse OM. Review study on household tumble driers - final report. 2019. doi: 10.13140/RG.2.2.34521.98407
32. Stawreberg L, Nilsson L. Modelling of specific moisture extraction rate and leakage ratio in a condensing tumble dryer. Applied Thermal Engineering. 2010; 30(14–15): 2173–2179. doi: 10.1016/j.applthermaleng.2010.05.031
33. Bassily AM, Colver GM. Performance analysis of an electric clothes dryer. Drying technology. 2003; 21(3): 499–524. doi: 10.1081/DRT-120018900
34. Bansal P, Islam S, Sharma K. A novel design of a household clothes tumbler dryer. Applied Thermal Engineering. 2010; 30(4): 277–285. doi: 10.1016/j.applthermaleng.2009.09.005
35. Shircliff M. Performance Prediction of Drying Process in Residential Clothes Dryer Using Multiphysics Modeling and Simulation. 2016. doi: 10.13140/RG.2.2.28164.35206
36. Lin Z, Wang H, Wang Y, et al. Experimental analysis on drying performance of a condensing clothes dryer with two new plate-fin heat exchangers. Case Studies in Thermal Engineering. 2023; 42: 102769. doi: 10.1016/j.csite.2023.102769
37. Ocharo HN, Komaki D. Quantifying potential power savings from household appliance consumption data: A methodological approach and estimated results. In: 2023 11th International Conference on Smart Grid (icSmartGrid). 2023: 322–327. doi: 10.1109/icSmartGrid58512.2023.00063
38. Novak L, Gatarić P, Širok B. Influence of drum inlet air conditions on drying process in a domestic tumble dryer. Drying technology. 2019; 37(6): 781–792. doi: 10.1080/07373937.2018.1461111
39. Plata S, Vicente W, Salinas-Vazquez M, Urbiola L. Analysis of the kinetic parameters of clothes drying in an electric vented dryer. Part II: Influence of the type of fabric. Drying Technology. 2023; 41(8): 1240–1251. doi: 10.1080/07373937.2022.2156538
40. Cummins AM, Malekpour AK, Smith AJ, Lonsdale S, Dean JR, Lant NJ. Impact of vented and condenser tumble dryers on waterborne and airborne microfiber pollution. PLoS One. 2023; 18. doi: 10.1371/journal.pone.0282759
41. Dietrich H. Heat pump patent, Deutsche Patent 3407439. 1984.
42. Rasti M, Hatamipour MS, Aghamiri SF, Tavakoli M. Enhancement of domestic refrigerator's energy efficiency index using a hydrocarbon mixture refrigerant. Measurement. 2012; 45(7): 1807–1813. doi: 10.1016/j.measurement.2012.03.034
43. Senthilkumar D. Influence of cryogenic treatment on tic nanopowder in R600a and R290 refrigerant used in vapor compression refrigeration system. International Journal of Air-Conditioning and Refrigeration. 2019; 27(04): 1950040. doi: 10.1142/S2010132519500400
44. Siddiqui MU, Owes A, Al-Amri FG, Saeed F. Recent Developments in the Search for Alternative Low-Global-Warming-Potential Refrigerants: A Review. International Journal of Air-Conditioning and Refrigeration. 2020; 28(03): 2030004. doi: 10.1142/S2010132520300047
45. Purwadianto D, Sugiharto B. Performance of Low Power Electric Energy Clothes Dryers for Households. International Journal of Applied Sciences and Smart Technologies. 2023; 5(1): 39–54. doi: 10.24071/ijasst.v5i1.6274
46. Patel VK, Boudreaux PR, Gluesenkamp KR. Validated model of a thermoelectric heat pump clothes dryer using secondary pumped loops. Applied Thermal Engineering. 2021; 184: 116345. doi: 10.1016/j.applthermaleng.2020.116345
47. TeGrotenhuis W, Butterfield A, Caldwell D, Crook A, Winkelman A. Modeling and design of a high efficiency hybrid heat pump clothes dryer. Applied Thermal Engineering. 2017; 124: 170–177. doi: 10.1016/j.applthermaleng.2017.06.025
48. Yamaguchi Y, Seii E, Itagaki M, Nagayama M. Evaluation of domestic washing in Japan using life cycle assessment (LCA). International Journal of Consumer Studies. 2011; 35(2): 243–253. doi: 10.1111/j.1470-6431.2010.00960.x
49. Boyano A, Cordella M, Espinosa N, et al. Ecodesign and Energy Label for Household Washing Machines and Washer Dryers. Luxembourg: Publications Office of the European Union; 2017. doi: 10.2760/686924
50. Denkenberger D, Calwell C, Beck N, Trimboli B, Driscoll D, Wold C. Analysis of Potential Energy Savings from Heat Pump Clothes Dryers in North America. Spokane: Ecova; 2013. doi: 10.13140/RG.2.2.19151.71845
51. Mahlia TMI, Hor CG, Masjuki HH, Husnawan M, Varman M, Mekhilef S. Clothes drying from room air conditioning waste heat: thermodynamics investigation. Arab J Sci Eng. 2010; 35(1).
52. Mancini F, Minetto S, Fornasieri E. Thermodynamic analysis and experimental investigation of a CO2 household heat pump dryer. International Journal of Refrigeration. 2011; 34(4): 851–858. doi: 10.1016/j.ijrefrig.2011.01.019
53. Patel VK, Gluesenkamp KR, Goodman D, Gehl A. Experimental evaluation and thermodynamic system modeling of thermoelectric heat pump clothes dryer. Appl Energy. 2018; 217: 221–232. doi: 10.1016/j.apenergy.2018.02.111

54. Sousa LHCD, Motta Lima OC, Pereira NC. Analysis of drying kinetics and moisture distribution in convective textile fabric drying. Drying Technology. 2006; 24(4): 485–497. doi: 10.1080/07373930600612027
55. Zhao J, Jian Q, Zhang N, Luo L, Huang B, Cao S. The improvement on drying performance and energy efficiency of a tumbler clothes dryer with a novel electric heating element. Applied Thermal Engineering. 2018; 128: 531–538. doi: 10.1016/j.applthermaleng.2017.09.053
56. Jian Q, Luo L. The improvement on efficiency and drying performance of a domestic venting tumble clothes dryer by using a heat pipe heat recovery heat exchanger. Applied Thermal Engineering. 2018; 136: 560–567. doi: 10.1016/j.applthermaleng.2018.03.036
57. Ahmadi M, Gluesenkamp KR, Bigham S. Energy-efficient sorption-based gas clothes dryer systems. Energy Convers Manag. 2021; 230: 113763. doi: 10.1016/j.enconman.2020.113763
58. Cao X, Zhang J, Li ZY, Shao LL, Zhang CL. Process simulation and analysis of a closed-loop heat pump clothes dryer. Applied Thermal Engineering. 2021; 199: 117545. doi: 10.1016/j.applthermaleng.2021.117545
59. Cay A, Tarakçıoğlu I, Hepbasli A. Exergetic analysis of textile convective drying with stenters by subsystem models: Part 1—Exergetic modeling and evaluation. Drying Technology. 2010; 28(12): 1359–1367. doi: 10.1080/07373937.2010.509709
60. Cay A, Tarakçıoğlu I, Hepbasli A. Exergetic analysis of textile convective drying with stenters by subsystem models: Part 2—Parametric study on exergy analysis. Drying Technology. 2010; 28(12): 1368–1376. doi: 10.1080/07373937.2010.498711
61. Yi T, Dye JC, Shircliff ME, Ashrafzadeh F. A New Physics-Based Drying Model of Thin Clothes in Air-Vented Clothes Dryers. IEEE/ASME Transactions on Mechatronics. 2016; 21(2): 872–878. doi: 10.1109/TMECH.2015.2506179
62. Huang XM, Zhao Y, Liu HQ. Simulation and experimental study on drying process of the household gas clothes dryer. Mathematical Problems in Engineering. 2019. doi: 10.1155/2019/7127672
63. Stawreberg L. Energy efficiency improvements of tumble dryers: Technical development, laundry habits and energy labelling. Karlstad: Karlstad University; 2011. Karlstad University Studies 2011:43. doi: 10.13140/RG.2.2.33292.95360
64. Li Z, Cheekatamarla PK, Shen B. Effect of air path heat losses at different locations in vapor compression-based clothes dryer. Quasi-steady modeling and design implications. Drying Technology. 2026: 1–16. doi: 10.1080/07373937.2025.2510531
65. Somdalen R, Köhler J. Theoretical investigation of a novel thermoelectric laundry dryer concept. Mater Today Proc. 2018; 5(4): 10323–10332. doi: 10.1016/j.matpr.2017.12.272
66. Jones CR, Corona A, Amador C, Fryer PJ. Dynamics of fabric and dryer sheet motion in domestic clothes dryers. Drying Technology. 2022; 40(10): 2087–2104. doi: 10.1080/07373937.2021.1947326
67. Mellmann J. The transverse motion of solids in rotating cylinders—forms of motion and transition behavior. Powder Technol. 2001; 118(3): 251–270. doi: 10.1016/S0032-5910(00)00402-4
68. Govender I. Granular flows in rotating drums: A rheological perspective. Miner Eng. 2016; 92: 168–175. doi: 10.1016/j.mineng.2016.03.014
69. Yu X, Cui Y, Ding X. Investigation on damage behaviors of cotton fabric in different fabric motion patterns during tumble-drying process. Drying Technology. 2023; 41(7): 1183–1198. doi: 10.1080/07373937.2022.2131818
70. Conde MR. Energy conservation with tumbler drying in laundries. Applied Thermal Engineering. 1997; 17(12): 1163–1172. doi: 10.1016/S1359-4311(97)00023-8
71. Toal R, Morgan R, McMullan JT. Experimental studies of low-temperature drying by dehumidification. Part 1—Apparatus and theory. International Journal of Energy Research. 1988; 12(2): 299–314. doi: 10.1002/er.4440120210
72. Toal R, Morgan R, McMullan JT. Experimental studies of low-temperature drying by dehumidification. Part 2—Experimental. International Journal of Energy Research. 1988; 12(2): 315–344. doi: 10.1002/er.4440120211
73. Hekmat D, Fisk WJ. Improving the Energy Performance of Residential Clothesdryers. Lawrence Berkeley National Lab.(LBNL), Berkeley, CA (United States); 1984. doi: 10.2172/5702587
74. Boudreaux P, Gluesenkamp KR, Patel VK, Shen B. Measurement and analysis of clothes dryer air leakage. Drying Technology. 2021; 39(14): 2105–2117. doi: 10.1080/07373937.2020.1824189
75. Spruit FPM. Model van een trommeldroger. Eindhoven: Eindhoven University of Technology, Department of Industrial Engineering and Management Science; 1988. EUT-BDK Report No. 30. doi: 10.13140/RG.2.2.31090.84162
76. Kadoya K, Ohrnichi Y, Hosokawa F, Yamamoto T, Ishihara T. Condensation-type Clothes Dryer with New Heat-exchanger Fan. National Technical Report. 1984; 30(5): 613–619.

77. Kim JK. An experimental study on the optimum design of sirocco fan by using Taguchi method. Transactions of the Korean Society of Mechanical Engineers B. 1999; 23(6): 761–768. doi: 10.22634/KSME-B.1999.23.6.761
78. Roy RK. Design of experiments using the Taguchi approach: 16 steps to product and process improvement. John Wiley & Sons; 2001. doi: 10.1002/0471654645
79. Shen CC, Lu JH. The performance of condenser under different vehicle speeds. International Journal of Air-Conditioning and Refrigeration. 2013; 21(02): 1350013. doi: 10.1142/S2010132513500130
80. Yousef K, Bolin C, Engeda A, Hegazy A. Experimental investigation of a refrigerant as a coolant of a power plant condenser. International Journal of Air-Conditioning and Refrigeration. 2014; 22(04): 1450024. doi: 10.1142/S2010132514500242
81. Enteria N, Yoshino H, Mochida A, et al. Performance test of desiccant heating, ventilating and air-conditioning system by using multiple tracer gas dilution method. International Journal of Air-Conditioning and Refrigeration. 2015; 23(04): 1550027. doi: 10.1142/S2010132515500277
82. Zhang Z, Gui N, Ge L, Li Z. Numerical study of particle mixing in a tilted three-dimensional tumbler and a new particle-size mixing index. Advanced Powder Technology. 2019; 30(10): 2338–2351. doi: 10.1016/j.apt.2019.07.001
83. Khalsa KPS, Sadhu S. Experimental study of domestic refrigerator performance improvement with evaporative condenser. International Journal of Air-Conditioning and Refrigeration. 2021; 29(02): 2150015. doi: 10.1142/S2010132521500156
84. Zolotarevskiy V, Gallo SC, Pereira MP, Barnett MR. Modelling of impeller-tumbler wear test with discrete element method. Wear. 2022; 510: 204509. doi: 10.1016/j.wear.2022.204509
85. Fontana É, Donca R, Mancusi E, Ulson de Souza AA, Guelli Ulson de Souza SMA. Mathematical modeling and numerical simulation of heat and moisture transfer in a porous textile medium. The Journal of The Textile Institute. 2016; 107(5): 672–682. doi: 10.1080/00405000.2015.1054140
86. Akyol U, Erhan Akan A, Durak A. Simulation and thermodynamic analysis of a hot-air textile drying process. The Journal of the Textile Institute. 2015; 106(3): 260–274. doi: 10.1080/00405000.2014.916074
87. Welti-Chanes J, Vergara-Balderas F, Bermudez-Aguirre D. Transport phenomena in food engineering: Basic concepts and advances. Journal of Food Engineering. 2005; 67. doi: 10.1016/j.jfoodeng.2004.05.031
88. Çengel YA, Ghajar AJ. Heat and Mass Transfer: Fundamentals and Applications. 4th ed. New York: McGraw-Hill Education; 2015.
89. ASHRAE Handbook—1985 Fundamentals. Atlanta, GA: American Society of Heating, Refrigerating and Air-Conditioning Engineers; 1985.
90. Tsilingiris PT. Combined heat and mass transfer analyses in solar distillation systems—The restrictive conditions and a validity range investigation. Solar energy. 2012; 86(11): 3288–3300. doi: 10.1016/j.solener.2012.09.004
91. Tsilingiris PT. Theoretical derivation and comparative evaluation of mass transfer coefficient modeling in solar distillation systems—the Bowens ratio approach. Solar Energy. 2015; 112: 218–231. doi: 10.1016/j.solener.2014.12.005
92. Collazo-Abreu PL, Morejón-Mesa Y, Fernández-Chuairey L, Vázquez-Alfonso Y. Mathematical and experimental models for the analysis of solar seed drying. Revista Ciencias Técnicas Agropecuarias. 2018; 27(1): 89–98.
93. Gu LD, Min JC, Tang YC. Effects of mass transfer on heat and mass transfer characteristics between water surface and airstream. International Journal of Heat and Mass Transfer. 2018; 122: 1093–1102. doi: 10.1016/j.ijheatmasstransfer.2018.02.052
94. Brummans LGM. Modeling of Ink Drying in Porous Media [PhD thesis]. Eindhoven: Eindhoven University of Technology; 2019. doi: 10.13140/RG.2.2.24764.67200
95. He Q, Li C, Xue J, Chen J. Modeling and simulation of isothermal process of natural gas pipeline drying with dehydrated air. Drying Technology. 2020; 38(11): 1400–1410. doi: 10.1080/07373937.2019.1653318
96. Buysse S. The dryer section of a paper machine: modelling and simulation [MSc thesis]. Delft: Delft University of Technology; 2021. doi: 10.13140/RG.2.2.31392.81923
97. Sabau AS, Contescu CI, Jellison GD, et al. Evaporation due to infrared heating and natural convection. Heat and Mass Transfer. 2020; 56(8): 2585–2593. doi: 10.1007/s00231-020-02869-y
98. Nienke T, Embrechts H, Kwade A, Eggerath D. Experimental and numerical investigation of the influence of nozzle design on the industrial convection drying of thin films. Drying Technology. 2021; 1–11. doi: 10.1080/07373937.2021.1929292
99. Chasiotis V, Tzempelikos D, Filios A. Evaluation of a Moisture Diffusion Model for Analyzing the Convective Drying Kinetics of Lavandula x allardii Leaves. Computation. 2021; 9(12): 141. doi: 10.3390/computation9120141

100. Glaskova T, Aniskevich A. Moisture absorption by epoxy/montmorillonite nanocomposite. Composites Science and Technologies. 2009; 69(15–16): 2711–2715. doi: 10.1016/j.compscitech.2009.08.007
101. Ghimire A. Basic Principles of Engineering. Morrisville, NC: Lulu Press; 2017.
102. Jiang Z, Xi Y, Gu X, Huang Q, Zhang W. Modelling of water vapour sorption hysteresis of cement-based materials based on pore size distribution. Cement and Concrete Research. 2019; 115: 8–19. doi: 10.1016/j.cemconres.2018.09.009
103. Krischer O, Kast W. Die wissenschaftlichen Grundlagen der Trocknungstechnik [The scientific principles of drying technology]. Berlin: Springer; 1987. doi: 10.1007/978-3-642-96566-9
104. Adapa PK, Schoenau GJ, Sokhansanj S. Performance study of a heat pump dryer system for specialty crops—Part 2: Model verification. International Journal of Energy Research. 2002; 26(11): 1021–1033. doi: 10.1002/er.835
105. Adapa PK, Schoenau GJ, Sokhansanj S. Performance study of a heat pump dryer system for specialty crops—part 1: development of a simulation model. International Journal of Energy Research. 2002; 26(11): 1001–1019. doi: 10.1002/er.834
106. Bergman TL, Lavine AS, Incropera FP, DeWitt DP. Introduction to heat transfer. John Wiley & Sons; 2011. doi: 10.1002/9781118135446
107. Bengtsson P, Berghel J, Renström R. Performance study of a closed-type heat pump tumble dryer using a simulation model and an experimental set-up. Drying technology. 2014; 32(8): 891–901. doi: 10.1080/07373937.2013.873469
108. Turner I, Mujumdar AS. Mathematical modeling and numerical techniques in drying technology. CRC Press; 1996. doi: 10.1201/9780367803616
109. Haghi AK. A Mathematical Model of theDrying Process. Acta Polytechnica. 2001; 41(3). doi: 10.14311/29
110. Bejan A, Dincer I, Lorente S, Miguel A, Reis H. Porous and complex flow structures in modern technologies. Springer Science & Business Media; 2004. doi: 10.1007/978-1-4757-4223-3
111. Lee KS, Yang B, Pyo SY, Kim HG, Lee DH, Kim SD. Drying performance of a tumbler dryer with condenser. Korean Journal of Chemical Engineering. 2006; 23(4): 658–662. doi: 10.1007/BF02706810
112. Stawreberg L, Nilsson L. Potential energy savings made by using a specific control strategy when tumble drying small loads. Appl Energy. 2013; 102: 484–491. doi: 10.1016/j.apenergy.2012.08.038
113. Jian Q, Zhao J. Drying performance analysis of a condensing tumbler clothes dryer with a unique water cooled heat exchanger. Applied Thermal Engineering. 2017; 113: 601–608. doi: 10.1016/j.applthermaleng.2016.11.073
114. Gluesenkamp KR, Boudreaux PR, Shen B, Goodman DK, Patel VK. Experimental Measurements of Clothes Dryer Drum Heat and Mass Transfer Effectiveness. Oak Ridge National Lab.(ORNL), Oak Ridge, TN (United States); 2018. doi: 10.2172/1435796
115. Lee BH, Sian RA, Wang CC. A rationally based model applicable for heat pump tumble dryer. Drying Technology. 2019; 37(6): 691–706. doi: 10.1080/07373937.2018.1469155
116. Granryd E, Melinder Å. Secondary refrigerants for indirect systems. Refrigerating Engineering, Granryd, KTH, Stockholm. 2005; 6: 2–6.
117. Gluesenkamp KR, Boudreaux P, Patel VK, Goodman D, Shen B. An efficient correlation for heat and mass transfer effectiveness in tumble-type clothes dryer drums. Energy. 2019; 172: 1225–1242. doi: 10.1016/j.energy.2019.01.053
118. Shen B, Gluesenkamp K, Bansal P, Beers D. Heat pump clothes dryer model development. International Refrigeration And Air Conditioning Conference. 2016. doi: 10.13140/RG.2.2.33622.91205
119. Huelsz G, Urbiola-Soto L, López-Alquicira F, Rechtman R, Hernández-Cruz G. Total energy balance method for venting electric clothes dryers. Drying Technology. 2013; 31(5): 576–586. doi: 10.1080/07373937.2012.752745
120. Prasertsan S, Saen-Saby P, Ngamsritrakul P, Prateepchaikul G. Heat pump dryer Part 1: Simulation of the models. International Journal of Energy Research. 1996; 20(12): 1067–1079. doi: 10.1002/(SICI)1099-114X(199612)20:12<1067::AID-ER203>3.0.CO;2-G
121. Krischer O, Kröll K. Die wissenschaftlichen grundlagen der trocknungstechnik. Springer-Verlag; 2013. doi: 10.1007/978-3-642-92648-6
122. Huang K. Statistical mechanics. John Wiley & Sons; 2008. doi: 10.1002/9780470711330
123. Bassily AM, Colver GM. Correlation of the area-mass transfer coefficient inside the drum of a clothes dryer. Drying Technology. 2003; 21(5): 919–944. doi: 10.1081/DRT-120021428
124. Cochran M, Goodnight J, Babin B, Eckels S. Condensing dryers with enhanced dehumidification using surface tension elements. Applied Thermal Engineering. 2009; 29(4): 723–731. doi: 10.1016/j.applthermaleng.2008.04.003

125. Smolsky BM, Sergeyev GT. Heat and mass transfer with liquid evaporation. International Journal of Heat and Mass Transfer. 1962; 5(10): 1011–1021. doi: 10.1016/0017-9310(62)90005-8
126. Kovacı T, Dikmen E, Şahin AŞ. Evaluation of heat mass performances for freeze drying of mint leaves. Journal of Food Processing and Preservation. 2022; 46. doi: 10.1111/jfpp.15920
127. Rasti M, Jeong JH. A Review of Models for Estimation of Moisture Evaporation Rate from Clothes Inside a Clothes Dryer. International Journal of Air-Conditioning and Refrigeration. 2021; 29(01): 2130001. doi: 10.1142/S2010132521300011
128. AHAM. Household Tumble Type Clothes Dryers. AHAM HLD-1-1992. Washington, DC: Association of Home Appliance Manufacturers; 1992.
129. AHAM. Household Tumble Type Clothes Dryers. AHAM HLD-1-2009. Washington, DC: Association of Home Appliance Manufacturers; 2009.
130. Yu X, Li Y, Ding X. Dynamics of cotton textile motion in a domestic tumble dryer and its effect on drying performance. Textile Research Journal. 2021; 91(7–8): 851–873. doi: 10.1177/0040517520961047
131. Yu X, Cao W, Ding X. The effects of fabric's mechanical properties on its motion and drying performance in a domestic tumble dryer. Drying Technology. 2021; 39(4): 528–547. doi: 10.1080/07373937.2020.1819823
132. Lee J, Yun C, Park CH. Effect of Fabric Characteristics and Drum Rotation Speeds on the Movements and Drying Performances of Clothes in a Tumble Dryer. Fibers and Polymers. 2022; 1–12. doi: 10.1007/s12221-022-4956-7
133. Yu X, Cao W, Wei Y, Ding X. Wrinkling mechanism of woven cotton fabrics during domestic tumble drying. Drying Technology. 2018; 36(9): 1098–1106. doi: 10.1080/07373937.2017.1386692
134. Wei Y, Gong RH, Ning L, Ding X. Enhancing the energy efficiency of domestic dryer by drying process optimization. Drying Technology. 2018; 36(7): 790–803. doi: 10.1080/07373937.2017.1355311
135. Chen-Yu JH, Emmel J. Comparisons of fabric care performances between conventional and high-efficiency washers and dryers. Fashion and Textiles. 2018; 5(1): 1–19. doi: 10.1186/s40691-018-0133-3
136. El Fil B, Garimella S. The state of the art in energy saving techniques for garment/textile drying. Drying Technology. 2022; 40(11): 2235–2250. doi: 10.1080/07373937.2022.2035837
137. Higgins L, Anand SC, Hall ME, Holmes DA. Effect of tumble-drying on selected properties of knitted and woven cotton fabrics: Part I: Experimental overview and the relationship between temperature setting, time in the dryer and moisture content. Journal of the Textile Institute. 2003; 94(1–2): 119–128. doi: 10.1080/00405000308630601
138. Bansal PK, Braun JE, Groll EA. Improving the energy efficiency of conventional tumbler clothes drying systems. International Journal of Energy Research. 2001; 25(15): 1315–1332. doi: 10.1002/er.763
139. Braun JE, Bansal PK, Groll EA. Energy efficiency analysis of air cycle heat pump dryers. International Journal of refrigeration. 2002; 25(7): 954–965. doi: 10.1016/S0140-7007(01)00085-4
140. Sian RA, Wang CC. Comparative study for CO2 and R-134a heat pump tumble dryer—A rational approach. International Journal of Refrigeration. 2019; 106: 474–491. doi: 10.1016/j.ijrefrig.2019.07.013
141. El Fil B, Garimella S. Modeling and validation of a commercial gas-fired tumble dryer. Applied Thermal Engineering. 2021; 195: 117231. doi: 10.1016/j.applthermaleng.2021.117231
142. Cranston J, Askalany A, Santori G. Efficient drying in washer dryers by combining sorption and heat pumping. Energy. 2019; 183: 683–692. doi: 10.1016/j.energy.2019.06.135
143. Zaman SU, Tao X, Cochrane C, Koncar V. E-textile systems reliability assessment—A miniaturized accelerometer used to investigate damage during their washing. Sensors. 2021; 21(2): 605. doi: 10.3390/s21020605